Financial Mathematics MSc Dissertation MTHM038, 2023/24

Option Pricing with Fourier Methods for Exponential Lévy Models

Daniil Vorontsov, ID 230807431

Supervisor: Dr Michael Phillips

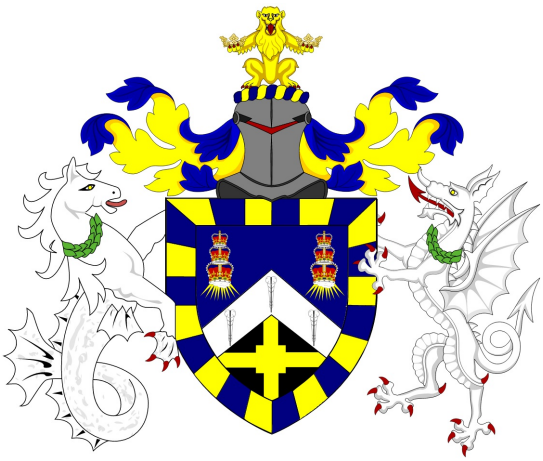

A thesis presented for the degree of
Master of Science in Financial Mathematics

School of Mathematical Sciences
and School of Economics and Finance
Queen Mary University of London

Declaration of original work

This declaration is made on September 2, 2024.

Student's Declaration: I, Daniil Vorontsov, hereby declare that the work in this thesis is my original work. I have not copied from any other students' work, work of mine submitted elsewhere, or from any other sources except where due reference or acknowledgement is made explicitly in the text. Furthermore, no part of this dissertation has been written for me by another person, by generative artificial intelligence (AI), or by AI-assisted technologies.

Referenced text has been flagged by:

1. Using italic fonts, **and**
2. using quotation marks "...", **and**
3. explicitly mentioning the source in the text.

To Grandpa Sergei, who motivated and supported me
throughout my entire education.

Abstract

The present thesis project is concerned with the subject of option pricing under Variance Gamma and CGMY processes as underlying models for stock price evolution. Both models belong to a family of jump processes, which are used as an alternative to traditional diffusion-based models (Black-Scholes, Heston). These models are of great interest since they are able to govern specific dynamics of infinite activity and/or of infinite variation. The family of jump processes, in turn, belongs to a wider class of exponential Lévy processes, which enable the use of the theory of stochastic processes to evaluate non-linear and path-dependent options. Another aim of the project is to study Fourier transform methods in the context of these models. The main advantage of these methods is greater performance compared with Monte Carlo simulation or even pricing via a semi-analytical formula which requires numerical integration. Three different approaches were revised and implemented: the well-known Carr-Madan formula, Fourier Space Time Stepping, and Fourier-cosine expansion. The first two approaches achieve great complexity reduction by employing the Fast Fourier Transform as shown in the work. Additionally, under the CGMY model two Monte Carlo methods were implemented and compared. The numerical part of the project was implemented in C++.

Contents

Chapter 1

Introduction

1.1 Background

Foundations of modern option pricing theory go back to the pioneering work of French mathematician Lois Bachelier [1]. As part of his doctoral thesis (1900), Bachelier proposed the first-ever model for the mathematical study of financial markets and applied it to a problem of nonlinear derivatives pricing. Five years before Einstein's famous 1905 paper on Brownian Motion[2], Bachelier derived the distribution function for what today is known as the Wiener process (an underlying stochastic process for Einstein's Brownian motion).

However, Bachelier's research did not receive substantial recognition during his lifetime. It is suggested[3, pp.10-11], the main reason is that by 1900 continental mathematics was highly inward-looking, focusing particularly on identifying rigorous methods. His supervisor, Henri Poincaré was forced to conclude that Bachelier's essay fell too far from the mainstream of French mathematics to be awarded the highest distinction[3, p.11]. Apparently, Einstein ignored Bachelier's work as well [4, pp. 213-214]. Nevertheless, due to efforts by Paul Lévy and Kolmogorov, his contribution to the theory of stochastic processes was recognized many years later. In the 1950s L.J. Savage and P. Samuelson reopened Bachelier's work, earning him the title of the forefather of mathematical finance[4, p.214].

Decades later, the Bachelier model provided the basis for a celebrated model of Fischer Black and Myron Scholes[5], which together with the work of Robert Merton[6] is known as Black-Scholes-Merton (BSM) framework (1973). Under BSM stock prices are driven by Geometric Brownian Motion (GBM), which is an extension of the Bachelier model, taking into account the non-negativity of stock prices. Closed-form analytical prices and the interpretability of their model provided great acknowledgment not only in the scientific world but also in the financial industry.

Despite having a number of benefits, the BSM market model requires a set of as-

sumptions, which limits its ability to capture real market behavior. The strongest is the assumption of constant volatility of underlying assets. This discrepancy results in the phenomenon called implied volatility smile due to empirical and predicted return distributions differing in terms of heavier tails and central peaks. To address this issue, a number of alternative models were suggested in the following decades. Among these asset models are Local Volatility models[7][8] which take as an input implied volatility obtained from actual market prices, therefore introducing a correction for BSM prices. Another approach is to introduce a separate correlated diffusion process for the volatility of the underlying asset, therefore creating a "volatility of volatility". This range of models is known as Stochastic Volatility models with Heston model[9] as its best-known example. However, these did not take into account events of isolated, sharp movements of stock prices. To incorporate them, several diffusion models with a jump component were presented[10][11], forming a Jump Diffusion model class.

In a Jump Diffusion model, the "normal" evolution of prices is given by a diffusion process, combined with jumps at random intervals. The jumps represent rare events: crashes and large drawdowns. Such an evolution can be represented by modeling the log price as a Lévy process with a nonzero Gaussian component and a jump part, which is a compound Poisson process with some given jump intensity. Another class of jump models consists of models with an infinite number of jumps in every interval, which are called infinite activity models. The intuition behind this comes from the fact that if the movements of stocks are examined on small time scales, it is clear that they do not resemble Brownian motion at all. They move in little jumps rather than continuously. The property of infinite activity produces dynamics of jumps rich enough to generate any nontrivial small-time behavior. Furthermore, we do not need to introduce a Brownian component. It has been argued[12][13][14] that such models give a more realistic description of the price process at various time scales. One of the first examples is Variance Gamma (VG)[15]. This model is derived by evaluating a Brownian motion with drift at random times that are driven by a Gamma process. The underlying concept is that the volatility should be a measure of a stock's sensitivity to information as it arrives and the amount of information arriving is random. Thus arriving information is described by a random process itself. We may think of trading volume as a proxy for information arrival. There is some statistical evidence that stock price returns are more log-normal when rescaled to use trading volume for the time parameter instead of calendar time[15]. Since VG is defined through SDE, its parameters come from the distribution of subordinated Gamma process and volatility of evaluated Brownian motion. Rather a general model was proposed by Carr, Geman, Madan, and Yor and named after them (CGMY) [14]. In CGMY stock evolution is defined through Lévy density which enables to switch process from infinite variation to finite variation by varying parameters.

1.2 Literature review

Despite being able to reproduce small-time behavior, many jump process models do not have closed-form solutions for European option prices, which is a serious drawback compared to BSM. The reason for this is that many processes with non-trivial jump dynamics do not exhibit a tractable density. In these cases, option pricing heavily relies on the Lévy–Khintchine theorem, which provides a link between characteristic function and the Lévy density, function, which defines the behavior of the jumps. Generally, by knowing the characteristic function, it is possible to derive pricing methods based on the Fourier transform, since the characteristic function is a Fourier image of the density function.

To tackle the issue of computational complexity when pricing options under non-BSM models, a new approach was proposed, beginning with Heston[9]. Rather than computing option prices directly by an analytical stochastic process, it is more efficient to map the characteristic function of the risk-neutral density, i.e. considering the problem in Fourier Space. It is well known, that calculations in Fourier space are often much easier than in the original domain. Such operations as taking derivative or convolution of functions in original space are replaced by multiplication by argument and dot product respectively. To obtain a solution for the original problem, the Fourier image function has to be inverted via inversion methods.

Bakshi and Chen[16] evaluate options numerically by employing Gil-Pelaez[17] inversion formula for the delta and risk-neutral probability of finishing in the money. An improvement was carried out by Carr and Madan in their paper[18] where they derived two novel approaches for option pricing that require single integration. Furthermore, their procedure could be run with the Fast Fourier Transform algorithm to price the option chain of different strikes simultaneously. Lewis[19] makes use of the Parseval formula, i.e. the property of Fourier transform which preserves the inner product and achieves a variety of valuation formulae utilizing Residual Calculus.

Lord, Fang, et al. developed the CONV method [20] based on a reformulation of the risk-neutral valuation formula by recognizing that it is a convolution. The resulting convolution can be dealt with numerically by utilizing the Fast Fourier Transform. A similar convolution-based approach was derived by Jackson et al., known as Fourier Space Time-stepping[21] (FST). The main idea is to solve the corresponding partial-integro differential equation (PIDE) in Fourier Space. Both of these approaches can be extended to price path-dependent options (American, Barrier, Bermudian, etc.). FST method can be accelerated by running on GPU[22].

Another prominent pricing method serving as a solid alternative to FFT-based pricing methods is the COS method developed by Fang and Oosterlee[23]. Rather than using the

Discrete Fourier Transform, they proposed to use Fourier-cosine expansion. It is known, that only even functions can be expressed as Fourier cosine series. Fang and Ooseterlee show that cosine expansion can be used on any function, defined on $[0, a]$, $a > 0$ by extending it to $[-a, a]$. One of the greatest advantages, claimed in the paper is that the convergence rate of the COS method is exponential and the computational complexity is linear, which makes it one of the most efficient methods up to today. Furthermore, later COS was adapted to run on GPU[24].

Recently, new applications of wavelet techniques started to appear in the context of option pricing. Matache et al.[25] proposed to use wavelets directly as part of the numerical discretization for the option pricing PDEs. Ortiz-Gracia and Oosterlee argue[26] that the COS method, although highly efficient, lacks robustness for a number of cases. The integration interval must be defined a priori, and the method also shows sensitivity in the choice of the interval for some models like CGMY. They considered the use of Haar wavelets as well as low-order B-spline wavelets instead of cosines in the COS method. They showed that the use of wavelets is robust in terms of sensitivity with respect to the size of the integration interval. They introduced an adaptive wavelet method, avoiding an apriori choice of the integration interval like in COS. Maree and the same authors later considered Shannon wavelets, based on the sinus cardinal (sinc) function[27]. They argued these are very interesting alternatives, possessing benefit from the local features of the density approximation, and giving exponential convergence of the method due to the regularity of the employed wavelet basis. This method is called SWIFT (Shannon Wavelet Inverse Fourier Technique) and allows robust and accurate pricing of long and short-term maturities together with fat-tailed asset price distributions.

For Variance Gamma prices authors derived a semi-analytical formula involving numerical integration with respect to conditional distribution. Later, they came up with a simplified formula for prices, reducing it to a combination of special functions[28]. This approach is similar to how European prices are derived under the Kou model[11]. Still, these formulae partially consist of numerical integration, thus making it difficult to maintain trading strategies due to the computationally costly calibration stage.

CGMY is a generalized VG process with parameters sourcing from the form of Lévy density. This specific way of defining process makes it impossible to do straightforward simulation by Monte Carlo or numerically integrate, like for Variance Gamma. Ballotta and Kyriakou [29] proposed an efficient Monte Carlo procedure, relying on a brute force approach consisting of sampling trajectories from density, recovered by inversion of characteristic function. Needless to say, there is no conventional solution for European options prices under CGMY, however recent works by Chen et al.[30] provide a semi-analytical formula with a reliable numerical evaluation technique.

Chapter 2

Lévy processes in Finance

This chapter attempts to provide a sufficient basis for the models studied in the present thesis. We revise some basic definitions and theorems from the stochastic processes theory and its applications in finance. For more extensive coverage, the reader is referred to [4, Chapters I, II] and [31, Chapters 1-6]. A very hands-on textbook by Cornelis Oosterlee[32] covers the same preliminaries and advanced material in simple language.

2.1 Black Scholes model

2.1.1 Brownian Motion

The first of the most popular and used stochastic processes with a great number of applications in finance, statistics, physics, and other sciences is Brownian Motion. For intuition behind Brownian Motion, we introduce a fair game:

- Each time interval Δt coin is flipped
- If the coin shows head, the player is granted with $\sqrt{\Delta t}$ amount of money
- If the coin shows tail, player lose $\sqrt{\Delta t}$ amount of money

Now for a game with $\sqrt{\Delta t} \to 0$ we define the player's funds at time t as W_t. This resulting process W_t is Brownian motion, sometimes referred to as the Wiener process, named after Norbert Wiener, who was the first to introduce its mathematical formulation.

Before formally defining Brownian motion, we first provide some essential stochastic theory definitions. Since conceptually, stochastic processes aim to facilitate the description and study of time-evolving random phenomena, regular probability space triplet $(\Omega, \mathcal{F}, \mathbb{P})$, which is typically defined for a single random variable, is enriched with **filtration**:

Definition 2.1. *A filtration on a given probability space* $(\Omega, \mathcal{F}, \mathbb{P})$ *is a collection of* σ*-algebras* $(\mathcal{F}_t, t \geq 0)$*, such that* $\forall t\ \mathcal{F}_t \subset \mathcal{F}$*, and* $\{\mathcal{F}_t\}_{t\geq 0}$ *is non-decreasing in the sense:*

$$\forall t_1 \leq t_2, \mathcal{F}_{t_1} \subset \mathcal{F}_{t_2}$$

This extension becomes more clear when we recall the purpose of **event space** $\mathcal{F}$, which is a set of events with each event being a set of outcomes from the **sample space** Ω. Given a **filtered probability space** $(\Omega, \mathcal{F}, (\mathcal{F}_t; t \geq 0), \mathbb{P})$, at any present time t, $\mathcal{F}_t$ should be understood as the σ-algebra of events observable up to time t. Without going deeper into measure theory, we conclude that filtration plays the role of "information", which expands as we move forward along the time scale. We will say process X_t is $\mathcal{F}_t$ - adapted if for any moment of time $t \geq 0$ the value of the process X_t is available at that same time, or rigorously, the random variable X_t is $\mathcal{F}_t$ - measurable [4, Section 2.4.2].

Definition 2.2 (Brownian motion). *Wiener process* $(W_t)_{t\geq 0}$ *is a* $\mathcal{F}_t$ *- adapted process, defined on filtered probability space, which satisfies the following properties:*

1. ***Starts at zero*** *almost surely (a.s.):* $W_0 = 0$
2. $(W_t)_{t\geq 0}$ *has a.s.* ***continuous paths***
3. ***Independent increments****: for any* $0 \leq s < t < \infty$*,* $W_t - W_s$ *is independent to* $\mathcal{F}_s$
4. *The increments are* ***stationary*** *and* ***normally distributed****:*
   for $0 \leq s < t < \infty$*,* $W_t - W_s \sim N(0, t-s)$

Third condition may be rewritten in the following formulation: for any increasing sequence of times $0 \leq t_0 < t_1 < ... \leq t_n < \infty$, the random variables W_{t_0}, $W_{t_1} - W_{t_0}$,..,$W_{t_n} - W_{t_{n-1}}$ are mutually independent. **Almost sure** in the first and second properties means the probability of such an event is one, i.e. $\mathbb{P}(W_0 = 0) = 1$.

2.1.2 Stochastic differential equations

The concept of stochastic processes provides with means to incorporate randomness into ordinary differential equations. The resulting **stochastic differential equation** governs the behavior of financial markets and can be used for pricing problems. If the source of randomness is Brownian Motion, we require process X_t to be adapted to filtration $\mathcal{F}_t$, generated by corresponding Brownian Motion W_t.

A common requirement in the pricing frameworks is the **Markovian** property of X_t. This means that at time s such that $0 \leq s < t$ process value X_t does not depend on the

information prior to s, but only on value X_s. X_t is said to be a Markovian process, if it satisfies:

$$\mathbb{E}[f(X_t)|\mathcal{F}_s] = \mathbb{E}[f(X_t)|X_s]$$

where $f(x)$ is any real-valued function, for which the expectations involved make sense.

A general SDE for some $\mathcal{F}_t$ - adapted Markovian process X_t with Brownian Motion as a noise source has the following form:

$$\begin{cases} dX_t = \mu\left(t, X_t\right) dt + \sigma\left(t, X_t\right) dW_t \\ X_0 = x_0 \end{cases} \tag{2.1}$$

Formulation 2.1 corresponds to the differential form of the equation and characterizes, in a formal way, the infinitesimal time-variation dX_t that is governed by a main "classical" force $\mu(t, X_t)dt$ and a "noise" $\sigma(t, X_t)dW_t$. Functions $\mu(t, X_t)$ and $\sigma(t, X_t)$ are known as **drift** and **diffusion** coefficients.

However, since the Wiener process **is not differentiable** in common sense, equation (2.1) is not to be understood like an ordinary differential equation. The differential form is just shorthand notation for writing

$$X_t = x_0 + \int_0^t \mu\left(s, X_s\right) ds + \int_0^t \sigma\left(s, X_s\right) dW_s \tag{2.2}$$

Through a combination of technical manipulations, the integrand in the second term in equation 2.2 could be approximated by a sequence of square-integrable simple processes (piecewise constant processes)[31, Section 4.2]. The resulting integral

$$\int_0^t \sigma\left(s, X_s\right) dW_s$$

is known as an **Itô integral**.

When drift and noise coefficients in SDE 2.1 does not depend on process values X_t, the solution to corresponding SDE is known as **Itô diffusion**:

Definition 2.3. *Process X_t is called Itô diffusion, if it satisfies the SDE of the form:*

$$\begin{cases} X_t = \mu_t dt + \sigma_t dW_t \\ X_0 = x_0, \quad x_0 \in \mathbb{R} \end{cases} \tag{2.3}$$

Where μ_t and σ_t are $\mathcal{F}_t$ - adapted processes submitted to integrability condition:

$$\int_0^t \left(|\mu_s| + \sigma_s^2\right) ds < \infty$$

Itô diffusion is a starting point for building calculus theory for stochastic processes. The following theorem takes central place:

Theorem 2.1 (Itô's lemma). *Let X_t be an Itô diffusion and function f(t,x) is differentiable in t and twice differentiable in x. Then f has a differential:*

$$df(t, X_t) = \left(\frac{\partial f}{\partial t} + \mu_t \frac{\partial f}{\partial x} + \frac{\sigma_t^2}{2}\frac{\partial^2 f}{\partial x^2}\right) dt + \sigma_t \frac{\partial f}{\partial x} dW_t \tag{2.4}$$

From the form of $df(t, X_t)$ it immediately follows that $f(t, X_t)$ is an Itô diffusion itself. This formula is a direct analog of the chain rule from classical calculus. If f is a function of t and some differentiable function $x(t)$, then:

$$df(t, x(t)) = f'(x(t))\frac{dx}{dt}dt + f'(x)dx$$

Both rules allow differential calculation of some arbitrary function f, which itself depends on some function X_t. However, in the stochastic version, extra terms are added to the differential part, associated with drift part dt. This difference is cleared through informal derivation. Following reasoning of [32, Section 2.1.2]:

Proof. (Informal) By expanding f into the Taylor series we obtain:

$$df = \frac{\partial f}{\partial t}dt + \frac{1}{2}\frac{\partial^2 f}{\partial t^2}dt^2 + \cdots + \frac{\partial f}{\partial x}dx + \frac{1}{2}\frac{\partial^2 f}{\partial x^2}dx^2 + \cdots$$

Substituting X_t for x and therefore $\mu_t dt + \sigma_t dW_t$ for dx gives

$$\begin{aligned} df = &\frac{\partial f}{\partial t}dt + \frac{1}{2}\frac{\partial^2 f}{\partial t^2}dt^2 + \cdots + \frac{\partial f}{\partial x}\left(\mu_t dt + \sigma_t dW_t\right) + \\ &+\frac{1}{2}\frac{\partial^2 f}{\partial x^2}\left(\mu_t^2 (dt)^2 + 2\mu_t\sigma_t dt dW_t + \sigma_t^2 \left(dW_t\right)^2\right) + \cdots \end{aligned}$$

In the limit $dt \to 0$ the terms dt^2 and $dtdW_t$ tend to zero faster than $(dW_t)^2$, which is $O(dt)$. Crossing out those and substituting dt for $(dW_t)^2$ (as a quadratic variation of a Wiener process[31, Section 3.4.2]), collecting the dt and dW_t terms, finally:

$$df = \left(\frac{\partial f}{\partial t} + \mu_t \frac{\partial f}{\partial x} + \frac{\sigma_t^2}{2}\frac{\partial^2 f}{\partial x^2}\right) dt + \sigma_t \frac{\partial f}{\partial x} dW_t$$

□

2.1.3 Black Scholes

Black and Scholes's paper[5] is celebrated due to its innovative approach to modeling share price dynamics. It may seem that Brownian motion is itself a good approximation of prices: prices move more or less independently relative to their past movement, it

is continuous at first approximation and increments exhibit somewhat normality. Nevertheless, the biggest disadvantage of this model is the positive probability of negative prices, which is never the case in the real world. To address this discrepancy, Black and Scholes proposed to use **Geometric Brownian Motion**(GBM):

Definition 2.4. *A stochastic process S_t is said to follow GBM if it satisfies the following stochastic differential equation:*

$$\begin{cases} dS_t = \mu S_t dt + \sigma S_t dW_t \\ S_0 = s, \quad s \in \mathbb{R} \end{cases} \tag{2.5}$$

By applying Itô's lemma, it is possible to show the following process is a solution to equation 2.5:

$$S_t = S_0 e^{(\mu - \frac{\sigma^2}{2})t + \sigma W_t} \tag{2.6}$$

Proof. Apply Itô's lemma 2.1 to process S_t given by 2.6. The diffusion in this case is Wiener process with drift $X_t = (\mu - \frac{\sigma^2}{2})t + \sigma W_t$ and function $f(t, X_t) = S_0 e^{X_t} = S_t$. The derivatives are straightforward to compute:

$$\begin{aligned} \frac{\partial f}{\partial x} =& \frac{\partial}{\partial x}(S_0 e^x) = S_0 e^x = f(t,x) \\ \frac{\partial^2 f}{\partial x^2} =& \frac{\partial}{\partial x^2}(S_0 e^x) = S_0 e^x = f(t,x) \\ \frac{\partial f}{\partial t} =& \frac{\partial}{\partial t}(S_0 e^x) = 0 \end{aligned}$$

Substituting derivatives into equation 2.4 yields:

$$\begin{aligned} df(t, X_t) =& \left[(\mu - \frac{\sigma^2}{2}) f(t, X_t) + \frac{\sigma^2}{2} f(t, X_t) \right] dt + \sigma f(t, X_t) dW_t = \\ =& \mu f(t, X_t) dt + \sigma f(t, X_t) W_t \end{aligned}$$

Recalling $f(t, X_t) = S_t$ and $df(t, X_t) = dS_t$:

$$dS_t = \mu S_t dt + \sigma S_t W_t$$

□

Since the exponential function e^x never reaches zero except at $x = \infty$, the GBM almost surely never hits zero. Sampled paths for stock price evolving according to GBM are presented in figure 2.1.

Definition 2.5. *Suppose we have a stock-bond market model. The stock price S_t is governed by some adapted process and bond price B_t is governed by $dB_t = rB_t d_t$. Assume*

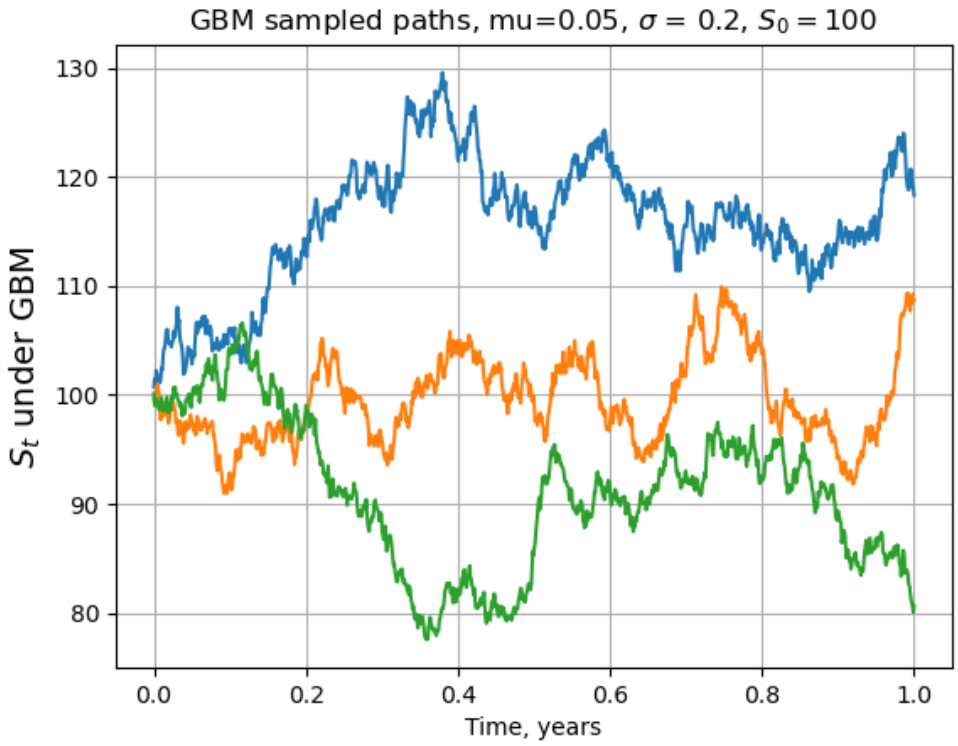

Figure 2.1: Sampled paths of stock price under GBM.

investors can trade the stock and invest in the bank, changing positions permanently. At time t the portfolio value X_t consist of:

- Δ_t *shares of stock, where* Δ_t *is an* $\mathcal{F}_t$ *- adapted process*
- $X_t - \Delta_t S_t$ *bond investments, growing continuously at constant rate* r

We will call X_t a self-financing strategy if at infinitesimal time step dt value of the portfolio changes as:

$$dX_t = \Delta_t dS_t + r(X_t - \Delta_t S_t)dt$$

The interpretation of this is that changes in portfolio value are only due to trading gains or losses, with no funds being added or withdrawn.

Black-Scholes (B-S) model is based on a set of strong assumptions about financial markets:

- There is one asset following GBM (share) and one asset growing at a constant rate (deposit)
- There are no dividends in the market
- Borrowing and lending cash can be done in any amount, including fractional
- Shares and derivatives can be traded in any amounts, including fractional and negative

- Trading occurs continuously
- The market is liquid and there are no transaction costs
- There is no arbitrage on the market

The assumption of no dividends can be relaxed. In practice, none of these assumptions holds. The model is only a distant approximation of what happens in the real world. Its simplicity and interpretability make it a good benchmark for further modifications.

Options are financial contracts, whose payoff depends on events related to the underlying asset. If the option payoff depends only on the final value of the asset, it is called a European style. Basic examples are European Call and Put.

Definition 2.6. *A European call option is a contract that gives the buyer of the contract the right, but not the obligation to buy a certain risky asset at a predetermined price K, at a predetermined time in the future, T. The payoff of this option is*

$$V_T = \max(S_T - K, 0) = (S_T - K)_+$$

Definition 2.7. *A European put option is a contract that gives the buyer of the contract the right, but not the obligation to sell a certain risky asset at a predetermined price K, at a predetermined time in the future, T. The payoff of this option is*

$$V_T = \max(K - S_T, 0) = (K - S_T)_+$$

When the current payoff of the European option is positive (e.g. at some time t $S_t - K > 0$ for the call or $K - S_t > 0$ for the put), we say the option is In The Money (ITM). When the reverse is true, the option is said to be Out of The Money (OTM).

By **arbitrage** we generally mean a possibility to create "something for nothing". In economic equilibrium, arbitrage should not exist, and requiring the absence of arbitrage strategies is a starting point of asset pricing.

Definition 2.8. *A self-financing strategy V_t is called an arbitrage opportunity, if for some $0 \leq T < \infty$:*

- *It requires zero initial investment:* $V_0 = 0$
- *Does not result in loss:* $\mathbb{P}(V_T \geq 0) = 1$
- *Makes profit with positive probability:* $\mathbb{P}(V_T > 0) > 0$

Link to option pricing comes through **First Fundamental Theorem of Asset Pricing** (FTAP-1):

Theorem 2.2 (FTAP-1). *The market model admits at least one risk-neutral probability measure $\mathbb{Q}$ equivalent to market measure $\mathbb{P}$ if and only if there is no arbitrage opportunity on the market.*

The measure $\mathbb{Q}$ is called equivalent to measure $\mathbb{P}$, if they have same null-sets:

$$\mathbb{Q}(A) = 0 \Leftrightarrow \mathbb{P}(A) = 0, \quad \forall A \in \mathcal{F}$$

Option pricing heavily relies on the existence of this measure as prices are obtained through risk-neutral valuation. The idea between risk-neutral probability is that market participants have different risk tolerance. To price an option, adjustment for every participant is required. By switching to another measure, we "enter" a world where all investors are **neutral** to risk. In such a world all discounted assets are martingales (expected value is current value). Therefore, any discounted option price is a martingale itself. The relation between initial market measure $\mathbb{P}$ and $\mathbb{Q}$ is given by the Girsanov theorem.

Assume we have an option with an expiration time of T. Let our option price process is V_t. Under risk-neutral measure following is true:

$$V_t = e^{-r(T-t)}\mathbb{E}^{\mathbb{Q}}[V_T] \tag{2.7}$$

For the B-S model, it is possible to reduce the valuation problem to the Partial Differential Equation (PDE) by constructing **hedged** portfolio, i.e. free to the risk associated with share price movements[33, Section 15.6]. The share price value S_t is given by:

$$dS_t = \mu S_t dt + \sigma S_t dW_t^{\mathbb{P}}$$

Applying Itô's lemma to price process $V_t(t, S_t)$:

$$\begin{aligned} dV_t &= \frac{\partial V}{\partial t}dt + \frac{\partial V}{\partial S}dS_t + \frac{1}{2}\frac{\partial^2 V}{\partial S^2}(dS_t)^2 = \\ &= \left(\frac{\partial V}{\partial t} + \mu S_t \frac{\partial V}{\partial S} + \frac{1}{2}\sigma^2 S_t^2 \frac{\partial^2 V}{\partial S^2}\right) dt + \sigma S_t \frac{\partial V}{\partial S} dW_t^{\mathbb{P}} \end{aligned} \tag{2.8}$$

Next, we construct a self-financing hedged portfolio Π_t, consisting of one option and an amount of $-\frac{\partial V}{\partial S}$ stocks. Its value at time t:

$$\Pi_t = V_t - \frac{\partial V}{\partial S} S_t$$

With infinitesimal change given by:

$$d\Pi_t = dV_t - \frac{\partial V}{\partial S} dS_t$$

By substituting dV_t from 2.8 and dS_t in the last equation:

$$\begin{aligned} d\Pi_t &= \left(\frac{\partial V}{\partial t} + \mu S_t \frac{\partial V}{\partial S} + \frac{1}{2}\sigma^2 S_t^2 \frac{\partial^2 V}{\partial S^2}\right) dt + \sigma S_t \frac{\partial V}{\partial S} dW_t^{\mathbb{P}} \\ &- \frac{\partial V}{\partial S} S_t \left(\mu dt + \sigma dW_t^{\mathbb{P}}\right) = \left(\frac{\partial V}{\partial t} + \frac{1}{2}\sigma^2 S_t^2 \frac{\partial^2 V}{\partial S^2}\right) dt \end{aligned} \tag{2.9}$$

Under the no-arbitrage assumption, the hedged portfolio should grow at a risk-free rate. If it earned more than this return, arbitrageurs could make a riskless profit by borrowing money to buy the portfolio; if it earned less, it could make a riskless profit by shorting the portfolio and buying risk-free securities[33, p.332]:

$$d\Pi_t = r\Pi dt \tag{2.10}$$

By equating 2.9 and 2.10, we obtain the final equation, also known as the Black-Scholes PDE :

$$\frac{\partial V}{\partial t} + rS\frac{\partial V}{\partial S} + \frac{1}{2}\sigma^2 S^2 \frac{\partial^2 V}{\partial S^2} - rV = 0 \tag{2.11}$$

Given payoff V_T and boundary conditions depending on the payoff function, this parabolic PDE is well-posed and can be solved through the change of variables reducing it to a standard diffusion equation. For European Call and Put options, there are closed-form solutions.

Another approach to derive 2.11 is through the Feynman–Kac formula, which gives a link between parabolic PDE and expectations of stochastic processes of the form 2.7[34, Section 6.4].

The powerful property of the B-S market is its **completeness**. This means that every option admits **unique** price. The market can be complete only in case there is one unique risk-neutral measure. This proposition is called **Second Fundamental Theorem of Asset Pricing** (FTAP-2).

Theorem 2.3. *An arbitrage-free market is complete if and only if there exists a unique risk-neutral measure $\mathbb{Q}$ that is equivalent to market measure $\mathbb{P}$.*

Despite all the advantages of the presented model, it does not capture the fundamental features of real-world financial markets. Real market prices returns exhibit heavier tails and a higher peak compared to B-S predictions. This difference is due to the assumption of constant volatility σ in stock dynamics. Further researchers attempted to address this issue by introducing various models of non-constant volatilities.

2.2 Exponential Lévy models

An interesting class of models is a class of jump processes, whose dynamic is formed by small or large jumps, occurring on different time intervals. Two market models incorporating jump processes are Variance Gamma[15] and CGMY[14]. Like in the B-S model, the market consists of two assets: bond with price evolving according to $dB_t = rB_t dt$ and stock S_t which is now the exponential Lévy process:

$$S_t = S_0 e^{L_t}$$

2.2.1 Lévy processes

A Lévy process is a generalization of Brownian Motion. Its definition is very similar to that of Brownian Motion:

Definition 2.9 (Lévy processes). *$\mathcal{F}_t$ - adapted process $(L_t)_{t\geq 0}$ is called a Lévy process if it satisfies the following properties:*

1. ***Starts at zero** a.s. : $L_0 = 0$*
2. ***Continuity in probability**: $\forall \varepsilon > 0$ and $t \geq 0$ it holds that $\lim_{h\to 0} P\left(|L_{t+h} - L_t| > \varepsilon\right) = 0$*
3. ***Independent increments**: for any $0 \leq s < t < \infty$, $L_t - L_s$ is independent to $\mathcal{F}_s$*
4. *The increments are **stationary**: for $0 \leq s < t < \infty$, $L_t - L_s \overset{\mathrm{d}}{=} L_{t-s}$*

The letter d above the equality sign stands for equality in distribution. An important corollary from the definition is that for any $t \geq 0$ value L_t has **infinitely divisible** distribution.

Definition 2.10. *We say a random variable ξ has infinitely divisible distribution, if $\forall n \geq 2\ \exists Y_1, \ldots, Y_n - i.i.d.$, such that $\xi \overset{\mathrm{d}}{=} Y_1 + \cdots + Y_n$*

To put it simply, this property comes from the fact of increments being independent. This means that process value at any time moment can be expressed as the sum of increments:

$$L_t \overset{\mathrm{d}}{=} L_0 + (L_{\Delta t} - L_0) + (L_{2\Delta t} - L_{\Delta t}) + \cdots + (L_t - L_{t-\Delta t})$$

Here $(L_{\Delta t} - L_0), (L_{2\Delta t} - L_{\Delta t}), \ldots, (L_t - L_{t-\Delta t}) \overset{\text{iid}}{\sim} \mathcal{P}(\Delta t)$ - some distribution. Thus, for every t, L_t has an infinitely divisible distribution as it is a sum of i.i.d random variables. Conversely, for every infinitely divisible distribution $\mathcal{P}$ there exists a Lévy process with $L_t \sim \mathcal{P}$.

A **characteristic function** is a powerful tool in probability theory and it is used widely in stochastic processes theory and consequently, in option pricing.

Definition 2.11. *Characteristic function of random variable X is a complex-valued function $\phi(u)$ defined as:*

$$\phi_X(u) = \mathbb{E}\left[e^{iuX}\right] \tag{2.12}$$

Where $i = \sqrt{-1}$ is an imaginary unit.

Expanding equation 2.12 by definition of expectation, we may rewrite:

$$\phi_X(u) = \int_{-\infty}^{\infty} e^{iux} f(x)dx$$

Where $f(x)$ is a density of random variable X. From this form, it is seen that the characteristic function is a **Fourier transform** of the density function[4, Section 2.2.3]. The convention for Fourier transform here follows [35, p.221]:

$$\mathfrak{F}[f](u) = \int_{\mathbb{R}} e^{iux} f(x)dx$$

By employing a convolution property of Fourier transform, we may rewrite the definition for infinitely divisible distribution as:

$$\phi_\xi(u) = \phi_{Y_1+\cdots+Y_n}(u) = \phi_{Y_1}(u)\ldots\phi_{Y_n}(u) = (\phi_{Y_1}(u))^n$$

The last equality is true since $Y_1, \ldots, Y_n$ are i.i.d. random variables. Thus, for ξ to be infinitely divisible, it is sufficient for its characteristic function to be powered characteristic function of some distribution. This allows us to define **characteristic exponent** for the Lévy process:

Definition 2.12. *For any Lévy process L_t $\exists\psi_L : \mathbb{R} \to \mathbb{C}$ such that:*

$$\phi_{L_t}(u) = \mathbb{E}\left[e^{iuL_t}\right] = e^{t\psi_L(u)}$$

This results in distribution of L_t being determined by L_1:

$$\phi_{L_1}(u) = e^{\psi_L(u)} \Rightarrow \psi_L(u) = \log(\phi_{L_1}(u)) \Rightarrow \phi_{L_t}(u) = e^{t\log(\phi_{L_1}(u))}$$

Operating with Lévy processes provides an essential improvement compared to the Wiener process since they enrich dynamics with jumps. Generally, any Lévy process consists of three terms: drift, diffusion, and jumps. While the first two parts were already presented in GBM, information about jumps comes from the **Lévy measure**.

Definition 2.13. *Let $(L_t)_{t\geq 0}$ is a Lévy process with values in $\mathbb{R}$. We say the measure v on $\mathbb{R}$*

$$v(S) = \mathbb{E}\left[\#\{t \in [0,1] : \Delta L_t \neq 0, \Delta L_t \in S\}\right], \quad S \in \mathcal{B}(\mathbb{R})$$

is called the Lévy measure of L_t and $v(S)$ is the expected number of jumps whose size belongs to S per unit of time. $\mathcal{B}(\mathbb{R})$ is a Borel σ-algebra of a real line.

In total, any Lévy process is generated by a corresponding **Lévy triplet**: (μ, σ, v). μ is a corresponding drift term, σ is diffusion term and v is Lévy measure, producing jump term. For Brownian motion with constant drift and volatility, this triplet has form $(\mu, \sigma, 0)$. For Poisson process with jump intensity λ and Lévy measure $v(S) = \lambda \mathbf{1}_{\{1\in S\}}$ the corresponding triplet is $(0, 0, v)$. $\mathbf{1}_{\{1\in S\}}$ is an indicator function which equal 1 if $1 \in S$.

The following theorem provides a link between characteristic function and generating triplet for any Lévy process:

Theorem 2.4 (Lévy-Khinchine theorem). *Let $(L_t)_{t\geq 0}$ is a Lévy process with generating triplet (μ, σ, v). Then its characteristic exponent is given by:*

$$\psi_L(u) = iu\mu - \frac{1}{2}u^2\sigma^2 + \int_{\mathbb{R}} \left(e^{iux} - 1 - iux\mathbf{1}_{\{|x|\leq 1\}}\right) v(dx)$$

Where Lévy measure satisfies:

$$\int \min(1, x^2) v(dx) < \infty$$

Moreover, when the Lévy measure satisfies an additional condition

$$\int_{|x|\geq 1} |x| v(dx) < \infty$$

There is no need to truncate large jumps and the characteristic function has the form:

$$\psi_L(u) = iu\mu - \frac{1}{2}u^2\sigma^2 + \int_{\mathbb{R}} \left(e^{iux} - 1 - iux\right) v(dx)$$

Lévy processes with paths that exhibit jumps infinitely many times on a finite interval are called **infinite activity** jump processes[32, Section 5.3].

Definition 2.14. *Let $(L_t)_{t\geq 0}$ is a Lévy process with generating triplet (μ, σ, v)*

- *$(L_t)_{t\geq 0}$ is called a finite activity process if $v(\mathbb{R}) < \infty$*
- *$(L_t)_{t\geq 0}$ is called an infinite activity process if $v(\mathbb{R}) = \infty$*

Brownian motion, Poisson, Compound Poisson and Merton jump diffusion processes all belong to the finite activity Lévy processes, where paths typically consist of a contin-

uous Brownian motion component and/or a jump component. The jumps occur a finite number of times on each finite interval.

The next differentiation which is made in the case of Lévy processes is based on the notion of finite or infinite **variation**. We recall that the total variation of a function $f : [a, b] \to \mathbb{R}$:

$$TV(f) = \sup \sum_{i=1}^{n} |f(t_i) - f(t_{i-1})|$$

A Lévy process is said to be of finite variation if its trajectories are functions of finite variation with probability one[4, Section 3.5].

Theorem 2.5. *[32, Section 5.3] Let $(L_t)_{t\geq 0}$ is a Lévy process with generating triplet (μ, σ, v). $(L_t)_{t\geq 0}$ is*

- *a finite variation process if $\int_{|x|<1} |x|v(dx) < \infty$ **and** $\sigma = 0$*
- *an infinite variation process if $\int_{|x|<1} |x|v(dx) = \infty$ **or** $\sigma \neq 0$*

2.2.2 Variance Gamma

Variance Gamma process was proposed by Madan and Seneta[15] to overcome shortcomings of the B-S model. The process for stock price evolution is defined by time changing an independent Brownian motion with volatility σ and drift θ) by a tempered stable subordinator. The resulting process is the so-called *normal tempered stable process.* In the case of Variance Gamma the subordinator is a **Gamma process**:

Definition 2.15. *A Gamma process $X_t^G(\mu, \nu)$ is a stochastic process whose increments are independent Gamma distributed random variables:*

$$X_t - X_s \sim \Gamma(t - s, \mu, \nu), \quad 0 \leq s < t < \infty$$

Where density of Gamma distribution is given by:

$$f_{\Gamma(\tau,\mu,\nu)}(g) = \left(\frac{\mu}{\nu}\right)^{\frac{\mu^2\tau}{\nu}} \frac{g^{\frac{\mu^2\tau}{\nu}-1}e^{-\frac{\mu}{\nu}g}}{\Gamma(\frac{\mu^2\tau}{\nu})}$$

$\Gamma(\alpha)$ *is the Gamma function, given by:*

$$\Gamma(\alpha) = \int_0^\infty t^{\alpha-1}e^{-t}dt$$

Since Gamma distribution belongs to a class of infinitely divisible distributions, it can be shown that it is the Lévy process. Parameter μ is said to be the mean rate of X_t^G and we shall typically take it to be 1. ν is said to be the variance rate of X_t^G. The Variance Gamma is then defined as:

Definition 2.16. *A Variance Gamma process* $X_t^{VG}(\sigma, \nu, \theta)$ *is defined by substituting a Gamma process* $X_t^G(1, \nu)$ *for the time variable in a Brownian motion with drift* θ *and volatility* σ*:*

$$X_t^{VG}(\sigma, \nu, \theta) = \theta X_t^G(1, \nu) + \sigma W_{X_t^G(1,\nu)}$$

The resulting stock price evolution is complemented by additional drift based on the actual calendar time rather than the randomly drawn time μ:

$$S_t = S_0 e^{\mu t + X_t^{VG}(\sigma,\nu,\theta)}$$

A set of 3 sampled paths under Variance Gamma are presented in figure 2.2. Note the drastic contrast with GBM. Since the dynamics consist exclusively of jumps, the line represents sudden sharp movements.

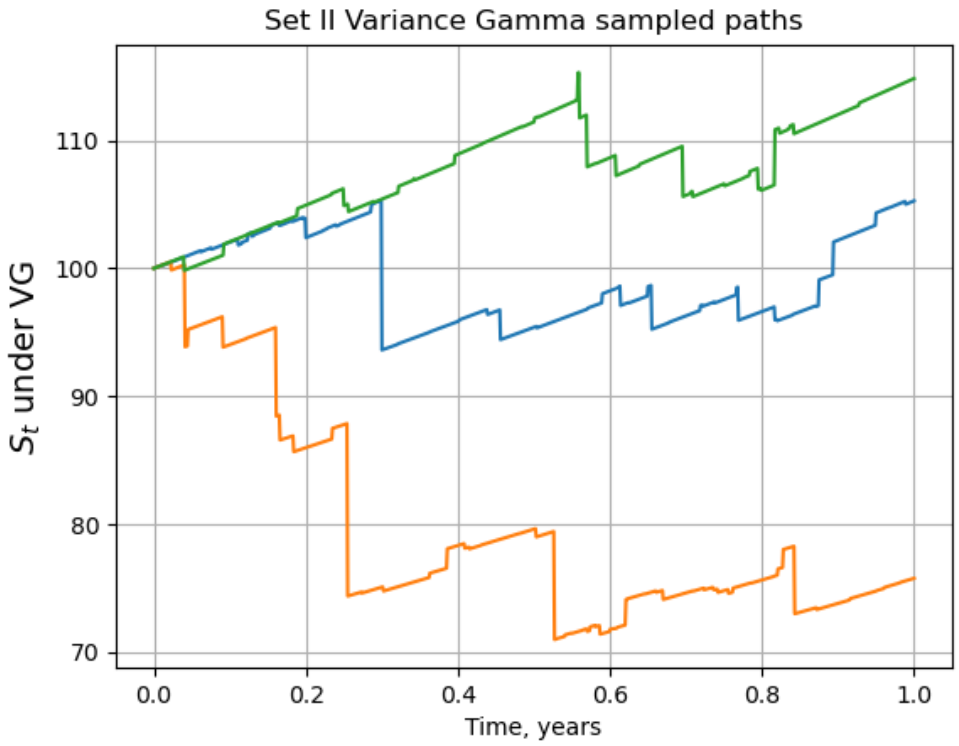

Figure 2.2: Sampled paths of stock price under VG. Parameters from set II (chapter 6)

One of the drawbacks of Variance Gamma compared to the B-S model is that the market is not complete anymore. While we still can find risk-neutral measure, it is not unique anymore. When we constructed a hedged portfolio for the B-S market, we relied on the idea of the possibility of hedging diffusion risk by purchasing $\Delta_t = \frac{\partial V}{\partial S}$ underlying assets. However, it is impossible to hedge risk, associated with jumps[4, Section 1.3]. We can therefore expect that a Variance Gamma model for stock movements will lead

to an incomplete market and therefore the existence of many risk-neutral measures. A common approach in this case is to change to a convenient probability measure and take the expectation of the discounted prices, like in risk-neutral valuation. It is denoted in a similar way to risk-neutral measure $\mathbb{Q}$ and is known in the Lévy literature as the **Equivalent Martingale Measure** (EMM).

Thus, one of the main issues in the context of Lévy asset price processes is to find a suitable EMM. Several methods to find an EMM have been proposed in the literature. One of them has been established in actuarial sciences, based on the Esscher transform with EMM condition written as[32, Section 5.3.3]:

$$e^{-rt}\mathbb{E}^{\mathbb{Q}}[S_t|\mathcal{F}_0] = S_0$$

Using $S_t = S_0 e^{L_t}$ we obtain:

$$S_0 e^{-rt}\mathbb{E}^{\mathbb{Q}}[e^{L_t}|\mathcal{F}_0] = S_0$$

Or:

$$\mathbb{E}^{\mathbb{Q}}[e^{L_t}|\mathcal{F}_0] = e^{rt} \tag{2.13}$$

By recalling the definition of the characteristic function, we change the left-hand side of equality with $\phi_{L_t}(-i)$:

$$\phi_{L_t}(-i) \overset{\text{def}}{=} \mathbb{E}^{\mathbb{Q}}[e^{-i^2 L_t}] = \mathbb{E}^{\mathbb{Q}}[e^{L_t}] = \mathbb{E}^{\mathbb{Q}}[e^{L_t}|\mathcal{F}_0] \tag{2.14}$$

Combining 2.13, 2.14, and Lévy - Khintchine representation theorem, we arrive at conditions for drift $\mu = r$ and for σ:

$$\frac{\sigma^2}{2} + \int_{\mathbb{R}} \left(\mathrm{e}^x - 1 - x\mathbf{1}_{|x|\leq 1}\right)\nu(dx) = 0$$

In the VG case, the characteristic function for X_t^{VG} is straightforward to obtain by recalling the characteristic function of the Gamma function[32, Section 5.4.1]:

$$\begin{aligned}\phi_{X_t^{VG}}(u) &= \mathbb{E}\left[\mathrm{e}^{iuX_t^{VG}}\right] \\ &= \mathrm{e}^{iu\mu t}\phi_{X_t^G}\left(u\theta + i\frac{1}{2}u^2\sigma^2\right) \\ &\overset{\text{def}}{=} \mathrm{e}^{iu\mu t}\left(1 - i\nu\theta u + \frac{1}{2}\nu\sigma^2 u^2\right)^{-\frac{t}{\nu}}\end{aligned} \tag{2.15}$$

To find the adjusted drift term, we substitute $u = -i$ into the resulting function:

$$\phi_{X_t^{VG}}(-i) = e^{-\mu t}\left(1 - \nu\theta - \frac{\nu\sigma^2}{2}\right)^{-\frac{t}{\nu}}$$

Now, by substituting the result into 2.13 one arrives at:

$$\mu t - \frac{t}{\nu}\log\left(1 - \nu\theta - \frac{\nu\sigma^2}{2}\right) = rt$$

Rewriting as $\mu = r + \bar{w}$, where the **convexity coefficient** reads

$$\bar{w} = \frac{1}{\nu} log\left(1 - \nu\theta - \frac{\nu\sigma^2}{2}\right)$$

By factoring quadratic expression in u in equation 2.15 VG process is decomposed as the difference of two Gamma processes.

$$\phi_{X_t^{VG}} = \mathrm{e}^{iu\mu t}\left(1 - i\eta_p u\right)^{-\frac{t}{\nu}}\left(1 + i\eta_n u\right)^{-\frac{t}{\nu}} \tag{2.16}$$

Where

$$\eta_p = \frac{\theta\nu}{2} + \sqrt{\frac{\theta^2\nu^2}{4} - \frac{\sigma^2\nu}{2}}$$
$$\eta_n = -\frac{\theta\nu}{2} + \sqrt{\frac{\theta^2\nu^2}{4} - \frac{\sigma^2\nu}{2}}$$

Under the risk-neutral measure, the drift changes to risk-free rate $\mu \to r$ and the characteristic function of the discounted process is just the product of two Gamma processes, representing "gains" $\mathcal{G}_t$ and "losses" $\mathcal{L}_t$.

$$\left(1 - i\eta_p u\right)^{-\frac{t}{\nu}}\left(1 + i\eta_n u\right)^{-\frac{t}{\nu}} = \phi_{\mathcal{G}_t}\phi_{\mathcal{L}_t}$$

By viewing the VG process as the difference between the two Gamma processes, it is possible to write the formula for its Lévy measure[15]:

$$v(dx) = \begin{cases} \frac{1}{\nu}\frac{e^{-M|x|}}{|x|}dx & \text{if } x > 0 \\ \frac{1}{\nu}\frac{e^{-G|x|}}{|x|}dx & \text{if } x < 0 \end{cases} \tag{2.17}$$

Where

$$M = \left(\sqrt{\frac{\theta^2\nu^2}{4} + \frac{\nu\sigma^2}{2}} + \frac{\theta\nu}{2}\right)^{-1}, \quad G = \left(\sqrt{\frac{\theta^2\nu^2}{4} + \frac{\nu\sigma^2}{2}} - \frac{\theta\nu}{2}\right)^{-1}$$

For European Call and Put options, it is possible to derive semi-analytical formula for the price C_0 as an integral over Black-Scholes prices. Conditioning X_t^{VG} on random

time X_t^G and applying tower property for expectations yields:

$$\begin{aligned} C_0 &= e^{-rT}\mathbb{E}[S_T] = e^{-rT}\mathbb{E}[S_0 e^{\mu T + X_T^{VG}}] = e^{-rT}\mathbb{E}[S_0 e^{(\bar{w}+r)T + X_T^{VG}}] \\ &= e^{-rT}\mathbb{E}[S_0 e^{(\bar{w}+r)T + \theta X_T^G + \sigma\sqrt{X_T^G}W_1}] = e^{-rT}\mathbb{E}\left[\mathbb{E}[S_0 e^{(\bar{w}+r)T+\theta g+\sigma\sqrt{g}W_1}|X_T^G = g]\right] \\ &= e^{-rT}\int_0^\infty f_\Gamma(g)\int_{-\infty}^\infty \varphi\left(S_0 e^{rT+\theta g+\bar{w}T+\sqrt{g}\sigma z}\right) f_{N(0,1)}(z)dzdg \\ &= e^{-rT}\int_0^\infty C_{BSM}(g) f_\Gamma(g)dg \end{aligned} \tag{2.18}$$

Here $\varphi(x)$ is payoff function and f_Γ, $f_{N(0,1)}$ are density functions of Gamma and standard normal distributions. Last equality follows from the fact that with fixed z, inner integral is payoff with stock following GBM. Therefore, this part can be rewritten in terms of B-S price.

$$C_{BSM}(g) = C_{BSM}(\tilde{S}_0(g), K, T, \tilde{\sigma}(g), r)$$

With $\tilde{S}_0(g) = S_0 e^{\theta g + wT + \frac{\sigma^2 g}{2}}$ and $\tilde{\sigma}(g) = \sqrt{\frac{g}{T}}$

2.2.3 CGMY

CGMY is essentially a generalization of a VG process defined in the previous section. In this case underlying Lévy model is parameterized through its Lévy measure:

$$v(dx) = \begin{cases} C\frac{e^{-M|x|}}{|x|^{1+Y}}dx & \text{if } x > 0 \\ C\frac{e^{-G|x|}}{|x|^{1+Y}}dx & \text{if } x < 0 \end{cases} \tag{2.19}$$

Lévy measure for CGMY differs from that of VG by the extra parameter Y accountable for various process properties. With $Y < 0$ we have a finite activity process. For $Y \in [0, 1]$ we deal with an infinite activity process of finite variation due to $\int_{|x|<1} xv(dx) < \infty$. When $Y \in (1, 2)$ the process is of infinite activity and infinite variation. We require the Lévy measure to be integrable with x^2 in the neighborhood of zero, which induces condition $Y < 2$. Other parameters are subject to $C \geq 0, G \geq 0, M \geq 0$.

The characteristic exponent for CGMY can be derived from the Lévy-Khintchine formula and is given by[32, Section 5.4.2]:

$$\psi_{X^{CGMY}}(u) = C\Gamma(Y)(M - iu)^Y - M^Y + (G + iu)^Y - G^Y) \tag{2.20}$$

Where Γ is the Gamma function, defined earlier.

While under VG there are semi-analytical formulae for European options and the Monte-Carlo procedure is straightforward, CGMY is a more complicated case. An equation analogous to the Black-Scholes PDE can be derived, incorporating a jump source,

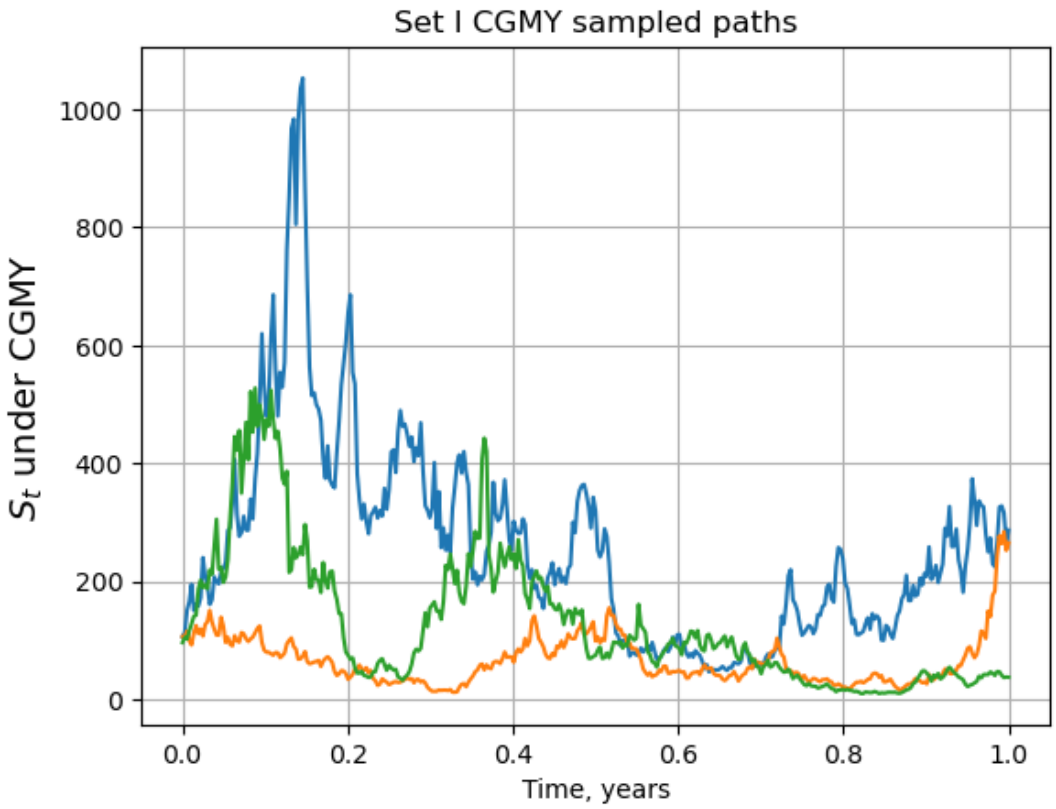

Figure 2.3: Sampled paths of stock price under CGMY. $S_0 = 100$, $r = 0.04$, $C = 1$, $G = 5$, $M = 5$, $Y = 1.8$

which results in a Partial Integro-Differential Equation (PIDE)[4, Chapter 12]. A common approach to solve it involves adopting Fractional Derivatives (FD) for the Implicit-Explicit scheme proposed by Cont-Voltchkova[36]. The differential part is discretized by an implicit scheme (similar to B-S PDE). The integral part is instead discretized by an explicit scheme. The reason for the explicit choice is that it avoids the inversion of the dense jump matrix. A blend of option pricing methods including a fractional partial differential equation and a partial integrodifferential schemes are considered in[37]. The results favored the COS method for European options over other FD approaches due to its accuracy and speed.

Chapter 3

Carr Madan inversion formula

Original Carr Madan paper[18] considers the problem of European call valuation with maturity T. As one of Fourier transform-based methods, option pricing is carried through the inversion of terminal payoff function. We begin by defining characteristic function of $s_T = log(S_T)$:

$$\phi_T(u) = [e^{ius_T}]$$

As discussed in the previous chapter, this characteristic function can be obtained from Lévy - Khintchine theorem or known analytically. Before the Carr-Madan paper, the common approach was to decompose option value C into two separate integrals:

$$C = S\Pi_1 - Ke^{-rT}\Pi_2$$

Where Π_1 is the delta of the option obtained through Gil-Pelaez inversion formula[17]:

$$\Pi_1 = \frac{1}{2} + \frac{1}{\pi}\int_0^\infty \mathrm{Re}\left[\frac{e^{-iu\ln(K)}\phi_T(u-i)}{iu\phi_T(-i)}\right]du$$

And Π_2 is the risk-neutral probability of an option finishing in the money:

$$\Pi_2 = \mathbb{P}\left(S_T > K\right) = \frac{1}{2} + \frac{1}{\pi}\int_0^\infty \mathrm{Re}\left[\frac{e^{-iu\ln(K)}\phi_T(u)}{iu}\right]du$$

One drawback is there is a need to compute two separate integrals. Another one is since u is in the denominator, the integrand is singular at $u = 0$, which makes the Fast Fourier Transform (FFT) not applicable. This is a major drawback, as the FFT is a well-used algorithm, which significantly speeds up computations. Carr Madan's formula addresses both of these issues.

3.1 Inversion formula

Let k denote the log of the strike price K, and let $C_T(k)$ be the desired value of a T maturity Call option with strike e^k. Risk-neutral density $q_T(s)$ of log price s_T is linked to its characteristic function ϕ_T through Fourier transform:

$$\phi_T(u) = \int_{\mathbb{R}} e^{ius} q_T(s) ds \tag{3.1}$$

Call value $C_T(k)$ is related to risk-neutral density as:

$$\begin{aligned} C_T(k) &= e^{-rT}\mathbb{E}\left[\max\left\{S_T - K, 0\right\}\right] \\ &= e^{-rT}\mathbb{E}\left[\left(e^{s_T} - e^k\right)_+\right] \\ &= e^{-rT}\int_{-\infty}^{\infty}\left(e^{s_T} - e^k\right)_+ q_T(s) ds \\ &= e^{-rT}\int_{k}^{\infty}\left(e^{s_T} - e^k\right) q_T(s) ds \end{aligned} \tag{3.2}$$

We note that at $K \to 0$, or $k \to -\infty$, $C_T(k)$ tend to S_0. Which makes the call function not square-integrable. To resolve this issue, a damping factor $\alpha > 0$ is introduced:

$$c_T(k) = e^{\alpha k} C_T(k) \tag{3.3}$$

The Fourier transform of $c_T(k)$ is given by:

$$\psi_T(v) = \int_{-\infty}^{\infty} e^{ivk} c_T(k) dk \tag{3.4}$$

Now, the original price is retrieved by inversion of $\psi_T(v)$:

$$C_T(k) = \frac{e^{-\alpha k}}{2\pi}\int_{-\infty}^{\infty} e^{-ivk}\psi_T(v) dv = \frac{e^{-\alpha k}}{\pi}\int_{0}^{\infty} e^{-ivk}\psi_T(v) dv \tag{3.5}$$

The second equality is valid because $C_T(k)$ is real which means $\psi_T(v)$ is odd in its imaginary part and even in its real part. Combining 3.1-3.4 it is possible to express $\psi_T(v)$ in terms of $\phi_T(v)$:

$$\begin{aligned} \psi_T(v) &= \int_{-\infty}^{\infty} e^{ivk}\int_{k}^{\infty} e^{\alpha k} e^{-rT}\left(e^s - e^k\right) q_T(s) ds dk \\ &= \int_{-\infty}^{\infty} e^{-rT} q_T(s)\int_{-\infty}^{s}\left(e^{s+\alpha k} - e^{(1+\alpha)k}\right) e^{ivk} dk ds \\ &= \int_{-\infty}^{\infty} e^{-rT} q_T(s)\left[\frac{e^{(\alpha+1+iv)s}}{\alpha + iv} - \frac{e^{(\alpha+1+iv)s}}{\alpha + 1 + iv}\right] ds \\ &= \frac{e^{-rT}\phi_T(v - (\alpha+1)i)}{\alpha^2 + \alpha - v^2 + i(2\alpha+1)v} \end{aligned} \tag{3.6}$$

Call values are obtained by substituting 3.6 into 3.5 and then carrying out the necessary integration. The equation 3.5 is a direct Fourier Transform, which enables the use of the FFT algorithm. The original paper does not provide specific guidance for the choice of damping coefficient α. It stipulates that for the modified call value to be integrable, $\psi_T(0)$ is required to be finite. From 3.6 this condition is equivalent to $\phi_T(-(\alpha+1)i)$ being finite. By definition of characteristic function:

$$\phi_T(-(\alpha+1)i) = \mathbb{E}[e^{-(\alpha+1)i^2 s_T}] = \mathbb{E}[S_T^{\alpha+1}] \tag{3.7}$$

Carr and Madan indicate $\alpha = 0.25$ showed reasonable results for convergence of their method for the VG model. However, only this condition does not narrow down the range for possible values for α.

The problem of optimal α values was studied in [38]. Two values of α were considered for the $\psi_T(v)$ function in 3.6 under B-S. The first value $\alpha_1 = \alpha_{minmax}$ was obtained by minimizing the maximum of the integrand in 3.5. The second value $\alpha_2 = 0.75$ was tested following results from [34]. With α_2 the inversion 3.5 resulted in significantly lower errors, which prompted the author to reject the proposed minimax strategy[38, Section 4.4].

In this project, α was tested for values in the range $[0.5, 10]$. Best value was picked for further comparison.

3.2 Discretization and FFT

To write discrete analog of equation 3.5, introduce grid $v_j = \eta(j-1)$, where η - step in Fourier space. The trapezoidal rule is written as:

$$C_T(k) \approx \frac{e^{-\alpha k}}{\pi}\eta\left[\sum_{j=1}^{N} e^{-iv_j k}\psi_T(v_j) - \frac{1}{2}\left[g(v_1) + g(v_N)\right]\right] \tag{3.8}$$

Where $g(v) = e^{-ivk}\psi_T(v)$. We recall the Discrete Fourier Transform (DFT):

$$F(k) = \sum_{n=1}^{N} e^{-\frac{2\pi i}{N}(n-1)(k-1)} f(n) \tag{3.9}$$

The most common and simplest FFT algorithm is a radix-2 decimation-in-time (**DIT**), which reduces the computation time of N sums of 3.9 from $O(N^2)$ to $O(N \log N)$. For log strikes, we introduce the following spacing:

$$k_u = -b + \lambda(u-1), \quad \text{for } u = 1, \ldots, N \tag{3.10}$$

Where $b = \frac{N\lambda}{2}$. Spacing in Fourier and spacing in real spaces are subject to Nyquist critical frequency constraint:

$$\lambda\eta = \frac{2\pi}{N} \tag{3.11}$$

Therefore, when η is chosen small enough to achieve a fine grid for the integration, we end up with relatively wide strike intervals with only a few strikes located in the range close to the stock price. By combining 3.8, 3.10 and 3.11, we arrive at:

$$C_T\left(k_u\right) \approx \frac{e^{-\alpha k_u}}{\pi}\eta\left(\sum_{j=1}^{N} e^{-i\frac{2\pi}{N}(j-1)(u-1)} e^{ibv_j}\psi_T\left(v_j\right) - \frac{1}{2}[g(v_1) + g(v_N)]\right)$$

Apart from the boundary term, we note FFT as in 3.9. To improve the accuracy of the integration with larger values η, Simpson's rule is used rather than the less precise Trapezoid rule:

$$C(k_u) = \frac{e^{-\alpha k_u}}{\pi}\frac{\eta}{3}\left(\sum_{j=1}^{N} e^{-i\frac{2\pi}{N}(j-1)(u-1)} e^{ibv_j}\psi(v_j)(3 + (-1)^j - \delta_{j-1}) - g_s\right)$$

Where δ_{j-1} is Kronecker delta which equals one at $j = 1$ and g_s is boundary condition:

$$g_s = g(v_{N-1}) + 4g(v_N)$$

The valuable result of the Carr Madan approach is that it enables to price of simultaneously the entire chain of options with log strikes in the range $[-b, b]$. However, under the constraint of the Nyquist frequency condition, there is a trade-off between eta and lambda. For most practical values of log strike spacing, the resulting range in Fourier space $[-b, b]$ is wide and a lot of obtained prices are not utilized.

Moreover, since the logarithmic grid for strikes rarely matches the desired chain of strikes, the interpolation step is required. Depending on the choice of interpolation algorithm, overall pricing time is increased.

Chapter 4

Fourier Space Time-Stepping

A distinct approach was introduced by Jackson et al[21]. Rather than inverting terminal payoff, Fourier Space Time-Stepping (FST) aims to solve the corresponding PIDE in Fourier Space. The following theorem is a key tool when constructing such PIDE for Lévy processes:

Theorem 4.1. *(**Lévy–Itô decomposition**) Let $(L_t)_{t\geq 0}$ is a Lévy process with Lévy measure ν satisfying:*

$$\int \min(1, x^2)v(dx) < \infty$$

$$\int_{|x|\geq 1} |x|v(dx) < \infty$$

Let J_X be a Poisson random measure of L_t, counting the number of jumps of size y occurring at time s. Its intensity measure is $\nu(dx)dt$. Then there exists $\mu \in \mathbb{R}$, $\sigma^2 \in \mathbb{R}$, and a Wiener process W_t such that:

$$\begin{aligned} L_t &= \mu t + \sigma^2 W_t + L_t^l + \lim_{\varepsilon \downarrow 0} \tilde{L}_t^\varepsilon, \qquad \textit{where} \\ L_t^l &= \int_{|x|\geq 1, s\in[0,t]} x J_X(ds \times dx) \qquad \textit{and} \\ \tilde{L}_t^\varepsilon &= \int_{\varepsilon \leq |x|<1, s\in[0,t]} x \left\{ J_X(ds \times dx) - \nu(dx)ds \right\} \\ &\equiv \int_{\varepsilon \leq |x|<1, s\in[0,t]} x \tilde{J}_X(ds \times dx). \end{aligned} \tag{4.1}$$

Lévy triplet (μ, σ, v), defined earlier, follows from this decomposition. L_t^l and $\tilde{L}_t^\varepsilon$ carries interpretation of large and small jumps correspondingly. In the case of a finite activity process there is no need to truncate small jumps and they can be combined with large jumps.

4.1 PIDE in Fourier Space

Let $V(t, X_t)$ be a discounted option price process under a risk-neutral measure. The share price is modeled by exponential Lévy process $X_t = S_0 e^{L_t}$, where L_t is subject to Lévy–Itô decomposition 4.1. $\varphi(x)$ is option payoff. Since $V(t, X_t)$ is a martingale under risk-neutral measure, we apply the zero-drift condition to arrive at the following PIDE:

$$\begin{cases} (\partial_t + \mathcal{L})\, V(t,x) = 0 \\ V(T,x) = \varphi\left(S_0 e^x\right) \end{cases} \tag{4.2}$$

Here $\mathcal{L}$ is the infinitesimal generator of the Lévy process that acts on twice differentiable functions $f(x)$ as follows:

$$\mathcal{L}f(x) = \left(\mu\partial_x + \frac{\sigma^2}{2}\partial_x^2\right) f(x) + \int_{\mathbb{R}/\{0\}} \left(f(x+\mathrm{y}) - f(x) - \mathrm{y}\cdot\partial_x f(x)\mathbf{1}_{|\mathrm{y}|<1}\right)\nu(d\mathrm{y})$$

∂_x is a differential operator. The convention for Fourier transform in this chapter follows the convention in the original paper[21]:

$$\mathfrak{F}[f](\omega) := \int_{-\infty}^{\infty} f(x) e^{-i\omega\cdot x} dx$$
$$\mathfrak{F}^{-1}[\hat{f}](x) := \frac{1}{2\pi}\int_{-\infty}^{\infty} \widehat{f}(\omega) e^{i\omega\cdot x} d\omega$$

Fourier transform $\mathfrak{F}$ is a linear operator mapping spatial derivatives ∂_x into multiplications in the frequency domain:

$$\mathfrak{F}\left[\partial_x^n f\right](t,w) = iw\mathfrak{F}\left[\partial_x^{n-1} f\right](t,w) = \cdots = (iw)^n \mathfrak{F}[f](t,w)$$

Consequently, applying the Fourier transform to the infinitesimal generator $\mathcal{L}f(x)$, allows the characteristic exponent to be factored out, according to Lévy–Khintchine theorem :

$$\begin{aligned} \mathfrak{F}[\mathcal{L}V](t,\omega) &= \left\{ i\mu\omega - \frac{\sigma^2}{2}\omega^2 + \int_{\mathbb{R}} \left(e^{i\omega y} - 1 - iy\omega\mathbf{1}_{|y|<1}\right)\nu(d\mathbf{y}) \right\} \mathfrak{F}[V](t,\omega) \\ &= \psi(\omega)\mathfrak{F}[V](t,\omega) \end{aligned} \tag{4.3}$$

Thus, taking the Fourier transform of both sides of the PIDE 4.2 leads to

$$\begin{cases} \partial_t \mathfrak{F}[V](t,\omega) + \psi(\omega)\mathfrak{F}[V](t,\omega) & = 0 \\ \mathfrak{F}[V](T,\omega) & = \mathfrak{F}[\varphi](\omega) \end{cases} \tag{4.4}$$

Equation 4.4 is an Ordinary differential equation (ODE) parameterized by ω. Given the

value of $\mathfrak{F}[V](T,\omega)$ at time $t_2 \leq T$, it is easily solved for t_1, such that $t_1 < t_2$:

$$\mathfrak{F}[V]\left(t_1,\omega\right) = \mathfrak{F}[V]\left(t_2,\omega\right)\cdot e^{\psi(\omega)(t_2-t_1)} \tag{4.5}$$

The solution is then inverted to return to the original space:

$$V\left(t_1,x\right) = \mathfrak{F}^{-1}\left\{\mathfrak{F}[V]\left(t_2,\omega\right)\cdot e^{\psi(\boldsymbol{\omega})(t_2-t_1)}\right\}(x) \tag{4.6}$$

4.2 FST method

Numerical implementation of the formula 4.6 is straightforward. In the case of European options, the procedure is similar in spirit to Carr Madan's inversion.

Considering a partition of the time and truncated stock price domain $\Omega = [0,T]\times[x_{min},x_{max}]$ into a finite mesh of points

$$\{t_m | m = 0,\ldots,M\}\times\{x_n | n = 0,\ldots,N-1\} \tag{4.7}$$

where $t_m = m\Delta t$, $x_n = x_{min} + n\Delta x$ and $\Delta t = \frac{T}{M}$, $\Delta x = \frac{x_{max}-x_{min}}{N-1}$.

Analogously, consider a partitioning of the time and frequency domain $\widehat{\Omega} = [0,T]\times[0,\omega_{\max}]$ into a finite mesh of points $\{t_m \mid m = 0,\ldots,M\}\times\{\omega_n \mid n = 0,\ldots,N/2\}$, where $\omega_n = n\Delta\omega$ and $\Delta\omega = 2\omega_{\max}/N$. Nyquist critical frequency in this case is $\omega_{\max} = \frac{1}{2\Delta x}$.

Let $V_n^m := V\left(t_m,x_n\right)$ represent $V(t,x)$ at the node points of the partition of Ω, and let $\hat{V}_n^m := \hat{V}\left(t_m,\omega_n\right)$ represent $\mathfrak{F}[V](t,\omega)$ at the node points of the partition $\widehat{\Omega}$. The frequency domain prices are obtained from the spatial domain prices as follows:

$$\begin{aligned}\hat{V}_n^m = \mathfrak{F}[V]\left(t_m,\omega_n\right) &\approx \sum_{k=0}^{N-1} V\left(t_m,x_k\right)e^{-i\omega_n x_k}\Delta x \\ &= \alpha_n \sum_{k=0}^{N-1} V_k^m e^{-ink/N} \\ &= \alpha_n \mathrm{FFT}\left[V^m\right](n)\end{aligned} \tag{4.8}$$

where $\alpha_n = e^{-i\omega_n x_{min}}\Delta x$ and $\mathrm{FFT}\left[V^m\right](n)$ denotes the n-th component of the discrete Fourier transform (DFT) of the vector V^m computed efficiently using the FFT algorithm. Applying the inverse Fourier operator to this equation, the spatial domain prices can be computed from frequency domain prices via a discrete

$$V_n^m = \mathrm{FFT}^{-1}\left[\alpha^{-1}\cdot\hat{V}^m\right](n).$$

Combining these connections between frequency and spatial domains with the transformed PIDE 4.6, a step backward in time is computed by

$$\begin{aligned} V^{m-1} &= \text{FFT}^{-1}\left[\alpha^{-1}\cdot\hat{V}^{m-1}\right] \\ &= \text{FFT}^{-1}\left[\alpha^{-1}\cdot\hat{V}^{m}\cdot e^{\psi\Delta t}\right] \\ &= \text{FFT}^{-1}\left[\alpha^{-1}\cdot\alpha\cdot\text{FFT}\left[V^{m}\right]\cdot e^{\psi\Delta t}\right] \\ &= \text{FFT}^{-1}\left[\text{FFT}\left[V^{m}\right]\cdot e^{\psi\Delta t}\right] \end{aligned} \tag{4.9}$$

Note that α coefficient representing spatial boundary cancels in the above equation and therefore omitted in numerical implementation.

European option is therefore concluded in one step, by setting $\Delta t = T$ and $V^T = \varphi(S_0 e^{x_n})$ in 4.9. Since partition $\{S_n\} = \{S_0 e^{x_n}\}$ does not necessarily include S_0, extra interpolation step is required.

When comparing 3.8 with 4.9 we anticipate greater time complexity of FST compared to Carr Madan method since there are now two FFT steps. Moreover, in Carr Madan FFT compute simultaneously a list of prices for options of different strikes, when output in FST method is a single price.

However, for 4.9 explicit expression of the Fourier transformed option payoff is not required anymore, which makes FST practical for non-standard payoffs. Furthermore, the FST method is easily generalized for path-dependent and American (with the possibility of early exercise) options.

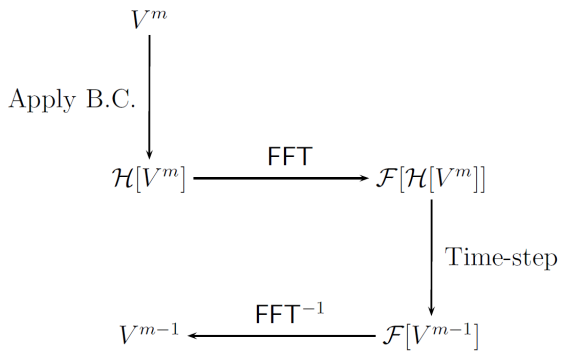

Figure 4.1: FST algorithm. The boundary conditions $\mathcal{H}$ are applied in real space while the time step is performed in Fourier space. Taken from[21]

Figure 4.1 provides the explicit procedure for path-dependent option pricing. $\mathcal{H}$ represents boundary conditions, such as optimal exercise or barrier breach. In case of American call option $\mathcal{H}$ is written as :

$$\mathcal{H}[V^m] = max(V^m, V^M)$$

In this project numerical implementation of 4.9 was based on the open-sourced sample from the author of the original paper [39]. The provided MATLAB code covers Black Scholes and Merton Jump Diffusion pricing models for European and American calls and puts. The code was adapted for C++ and adjusted for pure jump models, revised in Chapter 2.

Chapter 5

Fourier COS method

Both Carr Madan and FST methods rely on The Fourier transform, which expresses a general, non-periodic function as a continuous integral. However, integration techniques for solving Fourier transformed integrals require relatively fine grid since integrands for exponential Lévy models are usually highly oscillatory.

Fang and Oosterlee[23] proposed a different inversion approach, relying on Fourier-cosine series expansion, also called "cosine expansion". The main idea is to reconstruct the whole integral by extracting the series coefficients directly from the integrand.

5.1 Density recovery via Cosine expansion

The Fourier series represents a periodic function as a discrete sum of complex exponentials. The Fourier transform can be viewed as the limit of the Fourier series of a periodic function with the period approaching infinity.

For a function $f(x)$ supported on $[0, \pi]$ the Cosine expansion reads:

$$f(\theta) = \sum_{k=0}^{\infty}{}' A_k \cdot \cos(k\theta) \tag{5.1}$$

Where $\sum'$ indicates that the first term in the summation is weighted by one-half. The coefficients are given by:

$$A_k = \frac{2}{\pi} \int_0^{\pi} f(\theta) \cos(k\theta) d\theta$$

For function $f(x)$ supporterd on an arbitrary interval $[a, b]$ Fourier-cosine expansion is obtained via the change of variables:

$$\theta := \frac{x-a}{b-a}\pi; \quad x = \frac{b-a}{\pi}\theta + a$$

The expansion is given now by:

$$f(x) = \sum_{k=0}^{\infty}{}' A_k \cdot \cos(k\pi \frac{x-a}{b-a}) \tag{5.2}$$

With coefficients obtained through:

$$A_k = \frac{2}{b-a} \int_0^{\pi} f(\theta) \cos(k \frac{x-a}{b-a}) dx$$

In probability framework the density function $f_X(x)$ and characteristic function $\phi_X(u)$ form an example of a Fourier pair:

$$\phi_X(u)du = \int_{\mathbb{R}} e^{iux} f_X(x) dx$$

$$f_X(x) = \frac{1}{2\pi} \int_{\mathbb{R}} e^{-iux} \phi_X(u) du$$

Consider the interval $[a, b]$ such that truncated integral approximates characteristic function very well:

$$\tilde{\phi}_X(u) := \int_a^b e^{iux} f_X(x) dx \approx \int_{-\infty}^{\infty} e^{iux} f_X(x) dx = \phi_X(u) \tag{5.3}$$

Combining equation 5.2 with the cosine series coefficients of $f_X(x)$ on $[a, b]$ in 5.3 yields:

$$A_k \equiv \frac{2}{b-a} \operatorname{Re}\left\{ \tilde{\phi}_X \left(\frac{k\pi}{b-a} \right) \cdot \exp\left(-i \frac{ka\pi}{b-a} \right) \right\} \tag{5.4}$$

where $\operatorname{Re}\{\cdot\}$ denotes taking the real part of the argument. It then follows from 5.2 that $A_k \approx F_k$ with

$$F_k \equiv \frac{2}{b-a} \operatorname{Re}\left\{ \phi_X \left(\frac{k\pi}{b-a} \right) \cdot \exp\left(-i \frac{ka\pi}{b-a} \right) \right\} \tag{5.5}$$

We now replace A_k by F_k in the series expansion of $f_X(x)$ on $[a, b]$, i.e.

$$f_X(x) \approx \sum_{k=0}^{\infty}{}' F_k \cos\left(k\pi \frac{x-a}{b-a} \right) \tag{5.6}$$

and truncate the series summation such that

$$f_X(x) \approx \sum_{k=0}^{N-1}{}' F_k \cos\left(k\pi \frac{x-a}{b-a} \right) \tag{5.7}$$

The described procedure allows to recover any density function $f_X(x)$ given arbitrary characteristic function $\phi_X(u)$. There is need however to specify integration range $[a, b]$ and number of expansions N.

5.2 Option pricing with COS

The described procedure can be extended for option pricing. Let V_t is current option price written on share with current price $S_t = x$. Terminal price $S_T = y$ is distributed with risk-neutral density $f(y|x)$. First step is to truncate integral in risk-neural valuation:

$$\begin{aligned} V_t(x) = e^{-r(T-t)}\mathbb{E}^{\mathbb{Q}}[V_T] = e^{-r(T-t)}\int_{-\infty}^{\infty} V_T(y)f(y|x)dy \approx \\ \approx e^{-r(T-t)}\int_a^b V_T(y)f(y|x)dy \end{aligned} \tag{5.8}$$

Cosine expansion for density is written as:

$$f(y|x) = \sum_{k=0}^{\infty}{}' A_k(x)\cos\left(k\pi\frac{y-a}{b-a}\right) \tag{5.9}$$

So that

$$V_t(x) = e^{-r(T-t)}\int_a^b V_T(y)\sum_{k=0}^{\infty}{}' A_k(x)\cos\left(k\pi\frac{y-a}{b-a}\right)dy \tag{5.10}$$

Apply Fubini's Theorem to interchange the summation and integration, then introduce the following definition:

$$H_k := \frac{2}{b-a}\int_a^b V_T(y)\cos\left(k\pi\frac{y-a}{b-a}\right)dy \tag{5.11}$$

To write finally

$$V_t(x) = \frac{b-a}{2}e^{-r(T-t)}\sum_{k=0}^{\infty}{}' A_k(x)H_k \tag{5.12}$$

Similar to previous section, coefficients $A_k(x)$ are approximated by $F_k(x)$. Replacing $A_k(x)$ in 5.12 results in:

$$V_t(x) \approx e^{-r(T-t)}\sum_{k=0}^{N-1}{}' \mathrm{Re}\left\{\phi_{S_T}\left(\frac{k\pi}{b-a};x\right)e^{-ik\pi\frac{a}{b-a}}\right\}H_k \tag{5.13}$$

Here $\phi_{S_T}(u,x)$ is characteristic function of terminal share price S_T.

For European call and put options payoff function V_T is known. By switching to adjusted log-asset price $y_T = log(\frac{S_T}{K})$, it reads as:

$$V_T(y) := \left[\bar{\alpha}\cdot K\left(\mathrm{e}^y - 1\right)\right]^+ \quad \text{with} \quad \bar{\alpha} = \begin{cases} 1 & \text{for a call} \\ -1 & \text{for a put} \end{cases}$$

In this case, for range $a < 0 < b$ the integration in 5.11 yields:

$$\begin{aligned} H_k^{call} &= \frac{2}{b-a} K \left(\chi_k(0,b) - \psi_k(0,b) \right) \\ H_k^{put} &= \frac{2}{b-a} K \left(-\chi_k(a,0) + \psi_k(a,0) \right) \end{aligned} \tag{5.14}$$

Where χ and ψ are given by:

$$\psi_k(c,d) := \begin{cases} \left[\sin\left(k\pi \frac{d-a}{b-a} \right) - \sin\left(k\pi \frac{c-a}{b-a} \right) \right] \frac{b-a}{k\pi}, & k \neq 0 \\ d-c, & k = 0 \end{cases} \tag{5.15}$$

$$\begin{aligned} \chi_k(c,d) := & \frac{1}{1 + \left(\frac{k\pi}{b-a} \right)^2} \left[\cos\left(k\pi \frac{d-a}{b-a} \right) \mathrm{e}^d - \cos\left(k\pi \frac{c-a}{b-a} \right) \mathrm{e}^c \right. \\ & \left. + \frac{k\pi}{b-a} \sin\left(k\pi \frac{d-a}{b-a} \right) \mathrm{e}^d - \frac{k\pi}{b-a} \sin\left(k\pi \frac{c-a}{b-a} \right) \mathrm{e}^c \right] \end{aligned} \tag{5.16}$$

Given that the Cosine series expansion of entire functions converges exponentially, we can anticipate that equation 5.13 will provide highly accurate approximations for functions without singularities on the interval $[a, b]$, even with a small value of N.

Authors suggest cumulant functions for choosing truncation region:

$$[a,b] = \left[\zeta_1 - L_{COS} \sqrt{\zeta_2 + \sqrt{\zeta_4}}, \zeta_1 + L_{COS} \sqrt{\zeta_2 + \sqrt{\zeta_4}} \right] \tag{5.17}$$

for some value $L_{COS} > 0$. Cumulants are obtained from characteristic function by

$$\zeta_n(X) = \frac{1}{i^n} \frac{\partial^n \log(\phi_X(u))}{\partial u^n} \Big|_{u=0}$$

An alternative region, using only maturities [23]:

$$[a,b] = [-L_{COS}\sqrt{T}, L_{COS}\sqrt{T}] \tag{5.18}$$

Chapter 6

Numerical results

While the Carr Madan formula and COS method require parameter selection, the FST method is non-parametric. Under both Variance Gamma and CGMY models, the damping parameter α in Carr Madan was set at $\alpha = 1.5$, which provided the lowest errors under Variance Gamma. The integration range L_{COS} was different for VG and CGMY.

All three methods presented above were implemented and compared for European option pricing. They were compared in terms of speed and precision. Error analysis is presented with Maximum Absolute Error (MaxError) as target measure:

$$\text{MaxError} = \sup_{1 \leq i \leq 50} |\hat{C}(K_i) - C_i(K_i)|$$

Where $\hat{C}_i$ is price obtained by chosen method and C_i is reference price for given strike K_i. The computer used for tests has Intel(R) Core(TM) i5-11400H, 2.70 GHz with 12 CPU and RTX 3050 Ti Laptop GPU.

6.1 Variance Gamma

For VG reference prices were computed according to semi-analytical formula 2.18. Incomplete Gamma function provided with boost library[40] was utilized to speed up computations and to avoid divergence of Gamma density near $g = 0$.

6.1.1 Results

Two sets of parameters were considered. First set from Carr Madan paper[18] and second from COS paper [23]:

I. $S_0 = 100$, $r = 0.05$, $q = 0.03$, $T = 0.25$, $\theta = -0.1$, $\nu = 2$, $\sigma = 0.25$

II. $S_0 = 100$, $r = 0.1$, $q = 0$, $T = 1$, $\theta = -0.14$, $\nu = 0.2$, $\sigma = 0.12$

In total 50 European Call options were priced with strikes ranging from $K = 80$ to $K = 120$. The cubic spline library by Tino Kluge[41] was used for the interpolation step in Carr Madan (CM) and FST methods. For pricing times each method was run 10 times and the lowest value was used.

For Carr-Madan log-strike spacing was set at $\lambda = 0.0125$, damping parameter at $\alpha = 1.5$. For the COS method simple range of integration (equation 5.18) was used with $L_{COS} = 8$.

N	SET 1 pricing time (ms)				SET 2 pricing time (ms)			
	Analytical	CM	FST	COS	Analytical	CM	FST	COS
512		0.21	13	7		0.214	13	7
1024		0.423	27	14		0.432	27	14
2048	2139	0.85	55	27	1284	0.866	56	29
4096		1.751	115	55		1.767	116	57
8192		3.536	243	111		3.56	244	113

Table 6.1: Pricing time for 50 options in milliseconds for Fourier methods and analytical pricing (equation 2.18) under VG model.

While parameter variation did not affect the time performance of Fourier pricing methods, analytical pricing took almost twice as much time for set I.

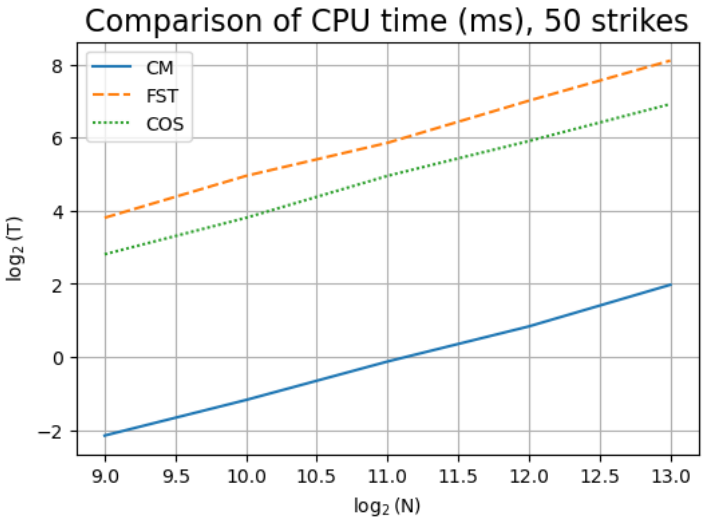

Figure 6.1: Pricing time under VG. Datapoints from Table 6.1. Set I.

This increase is caused by greater variation of a subordinate process $\frac{T}{\nu}$, which results in a sharp peak of the integrand in equation 2.18 near zero. Default policy allows Boost library to vary approximation used to result in the lowest level of error. Also, Boost may promote internally precision of data types (floats to doubles, doubles to long doubles) which might cause a longer evaluation time[42].

Figures 6.2 - 6.4 display error plots for different methods under the VG model. It can be seen on the plots for set I how $\frac{T}{\nu}$ affects the convergence of different methods. At $N = 2^{10} = 1024$ CM exhibits a constant shift from reference values, with peaks near spot strike.

Figure 6.2: Error plot for VG model. Number of expansion terms N = 1024. Reference price by formula 2.18. Set I.

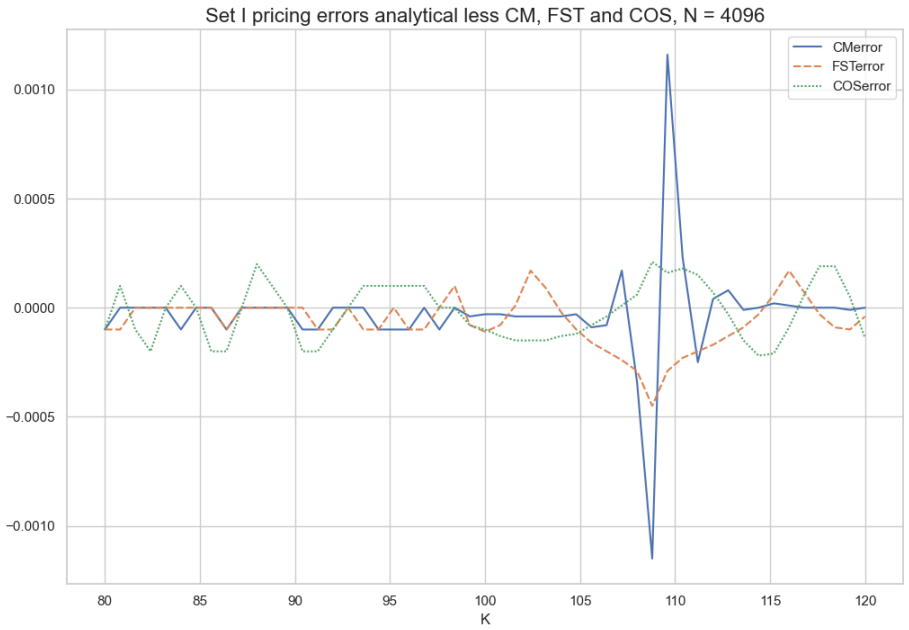

Figure 6.3: Error plot for VG model. Number of expansion terms N = 4096. Reference price by formula 2.18. Set I.

Figure 6.4: Error plot for VG model. Number of expansion terms N = 1024. Reference price by formula 2.18. Set II

The COS method outperforms others in terms of precision-runtime ratio. Despite having slower convergence for set I, it takes the same time as FST to achieve better precision, e.g. at N=1024 COS ran for 14 ms with MaxError of 0.01391 while FST at N=512 ran for 13 ms with MaxError of 0.04218 as can be seen in tables 6.1 and 6.2.

N	SET1			SET2		
	CM	FST	COS	CM	FST	COS
512	0.25	0.04218	0.11346	0.2594	0.02041	0.00001
1024	0.00335	0.00612	0.01391	0.00230	0.00514	0.00000
2048	0.00116	0.00315	0.00177	0.00000	0.00137	0.00000
4096	0.00116	0.00045	0.00022	0.00001	0.00033	0.00000
8192	0.00116	0.00010	0.00015	0.00001	0.00010	0.00000

Table 6.2: Max errors for different Fourier methods under VG model. In total 50 strikes.

CM MaxError does not decrease after $N = 2048$ with the minor increase for set II at $N = 4096$ and $N = 8192$. Possible explanation could be inferred by taking into account the interpolation step. Different combinations of log strike spacing λ and number of expansions N result in different interpolation points and their numbers. It is clear that CM does not benefit from a higher value of N with other parameters constant.

The FST method demonstrates consistent reduction in MaxError but requires more time to converge. FST requires an interpolation step like CM, but it does not encounter the same difficulty as interpolation is done on the spot price grid rather than on a strike grid. The x_{min} and x_{max} values in partitioning for FST (equation 4.7) are picked manually, which allows partition $\{S_n\} = \{S_0 e^{x_n}\}$ to include more "relevant" values, closer to S_0. Thus, interpolation is of higher efficiency than in CM.

6.2 CGMY

For CGMY reference prices were computed by the COS method with a reliable number of expansions $N = 2^{14}$ (COS extended). Two additional Monte-Carlo methods were implemented and compared with Fourier methods.

Since there is no trackable density for CGMY, direct simulation of the share price is impossible. However, all is not lost, since it is possible to recover the Cumulative Distribution Function (CDF) from characteristic function numerically through Fourier inversion and sample increments with Inverse transform sampling. This is known as "brute" approach.

A method to approximate so-called regularized CDF for CGMY by Fourier inversion is described in[29]. However, given the remarkable performance of the COS method in option pricing, the question of its validity for Monte Carlo sampling presents interest. The COS-based Monte Carlo sampling is denoted as MCFT-1 (Monte Carlo Fourier Transform) and regularized Fourier-based sampling is denoted as MCFT-2 correspondingly.

6.2.1 MCFT-1

Armed with density f_{X_T}, recovered via 5.7, the CDF values for given grid $\{x_j\}_{x=1}^{N}$:

$$F_{X_T}(x_n) = \int_{-\infty}^{x_n} f_{X_T}(z)dz \approx \sum_{j=0}^{n} f_{X_T}(x_j)\Delta x \tag{6.1}$$

Here $[x_0, x_N] = [x_{min}, x_{max}]$ is range for smallest and largest jumps. The Inverse sampling transform is then applied to obtain sampled $\hat{x}$:

$$\hat{x} = F_{X_T}^{-1}(U) \tag{6.2}$$

Where $U \sim \text{Unif}[0, 1]$. The intuition behind 6.2 is that since uniform values U lie between $[0, 1]$, they can serve as sampled "probabilities" of X_T being of size $\hat{x}$. Since sampled

values U do not necessarily lie on a grid $\{x_j\}_{x=1}^{N}$, the interpolation is required[29]:

$$\hat{x} = \begin{cases} x_0, & \text{if } U < F_0 \\ \frac{U\Delta x + x_i F_{l+1} - x_{l+1} F_l}{F_{l+1} - F_l}, & \text{if } F_l \leq U < F_{l+1} \text{ for } 0 \leq l < N \\ x_N, & \text{if } U \geq F_N \end{cases} \tag{6.3}$$

The Monte Carlo pricing then consists of several steps. First one is to sample M paths of terminal price $\hat{S}_T = e^{\hat{x}}$ and to compute M option payoffs $\hat{V}_T$. The price is obtained through the discounted average of these payoffs:

$$V_0 = \frac{e^{-rT}}{M} \sum_{j=1}^{M} \hat{V}_{T,j} \tag{6.4}$$

6.2.2 MCFT-2

One of the drawbacks of density recovery through COS method is the problem of range integration. While it is suggested that $L = 10$ in 5.18 provides high precision for most cases[32, Section 6.2.4], under CGMY this is not always the case. One also has to consider carefully the real space range $[x_{min}, x_{max}]$, as density has different supports for different parameters. A short region may result in biased samples due to the tails being "cut". However, since the COS method treats density as a periodic function, a wider region may result in a redundant signal as can be seen in figure 6.5.

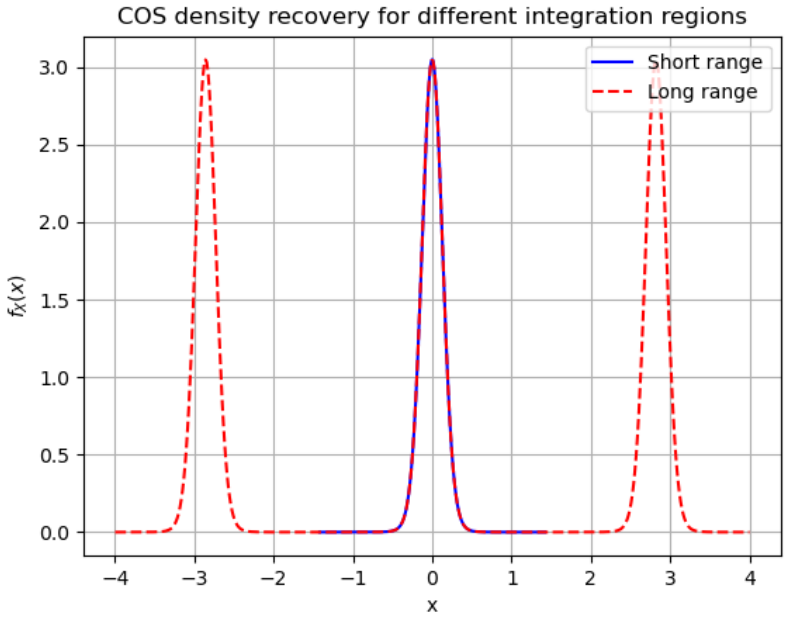

Figure 6.5: Recovered signal for CGMY density. Two ranges $[x_{min}, x_{max}]$: $[-8, 8]$, $[-1.5, 1.5]$

An alternative to COS method is to use the regularized CDF $F_r(x)$:

$$F_r(x) = F(x) - \frac{1}{2}F(x-D) - \frac{1}{2}F(x-D) \tag{6.5}$$

which is regularized in the sense that it decays to zero as $|x| \to \infty$. Then, for sufficiently large D, $F(x)$ approaches $F_r(x) + 1/2$ for fixed x. Hence, providing that $F_r(x)$ is known, it can be used to compute $F(x)$. The link between characteristic functions of regularized and regular CDF is given by [29]:

$$\phi_r(u) := \int_{\mathbb{R}} e^{iux} F_r(x)dx = \begin{cases} -\frac{1-\cos(uD)}{iu}\phi(u) & u \neq 0 \\ 0 & u = 0 \end{cases} \tag{6.6}$$

For integration range in real world $[-D/2, D/2]$ and range in Fourier space $[-L/2, L/2]$, the grid is given by $\{u_j\} = \{(j - \frac{N}{2})h\}_{j=0}^{N-1}$ and $\{x_l\} = \{(l - \frac{N}{2})\eta\}_{j=0}^{N-1}$ with $h = \frac{L}{N}$ and $\eta = \frac{D}{N}$. Regularized CDF is obtained through Fourier inversion:

$$F_r(x_l) = \frac{1}{2\pi}h\sum_{j=0}^{N-1} e^{-iu_j x_l}\phi_r(u_j) = \frac{1}{2\pi}he^{-iu_0(x_l - x_0)}\sum_{j=0}^{N-1} e^{-ijlh\eta}e^{-iu_j x_0}\phi_r(u_j) \tag{6.7}$$

Finally, CDF is calculated as

$$F(x_l) = F_r(x_l) + \frac{1}{2}$$

And sampled increments $\hat{x}$ are obtained in the same way as in the COS method through inversion 6.2 and interpolation 6.3.

Algorithm 1 MCFT-1 algorithm for Put option pricing

Input: Number of paths M, characterisitc funcion ϕ_{X_T}
Output: Option price V_0

```
f_{X_T} ← COS(φ_{X_T})        ▷ Equation 5.7
F_{X_T} ← f_{X_T}
V_0 ← 0
for m ← M to 1 do
    u ← U ~ Unif[0, 1]
    x̂ ← F^{-1}_{X_T}(u)       ▷ Equation 6.3
    V̂_T ← max(K − e^{x̂}, 0)
    V_0 ← V_0 + (e^{−rT}/M) V̂_T
end for
return V_0
```

Algorithm 2 MCFT-1 algorithm for Put option pricing

Input: Number of paths M, characterisitc funcion ϕ_{X_T}
Output: Option price V_0

```
φ_{r,X_T} ← φ_{X_T}           ▷ Equation 6.6
F_{r,X_T} ← φ_{r,X_T}         ▷ Equation 6.7
F_{X_T} ← F_{r,X_T} + 1/2
V_0 ← 0
for m ← M to 1 do
    u ← U ~ Unif[0, 1]
    x̂ ← F^{-1}_{X_T}(u)       ▷ Equation 6.3
    V̂_T ← max(K − e^{x̂}, 0)
    V_0 ← V_0 + (e^{−rT}/M) V̂_T
end for
return V_0
```

6.2.3 Monte Carlo on GPU

The Monte Carlo pricing involves generating many independent simulations of asset price paths. Since each path is independent of the others, they can be computed in parallel without any connections between them during the simulation phase. This is the reason, the Monte Carlo pricing method is known as **embarrassingly parallelizable** task.

The GPU part of the project was implemented in the CUDA framework. CUDA is a programming model, developed by Nvidia and hosted for Nvidia graphic processing units. CUDA operates with **kernels** - functions that are executed on GPU. The parallel part of applications is executed K times in parallel by K different CUDA threads, as opposed to only one thread in the CPU[43]. Each thread is assigned a unique global ID through the built-in variables.

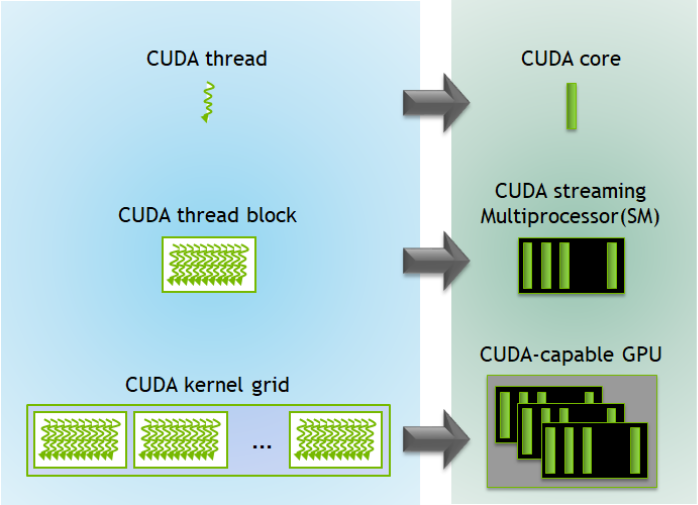

Figure 6.6: Kernel execution on GPU[43]

A set of threads is organized into a **block**, and multiple blocks together form a **grid**. A kernel is executed as a grid of blocks of threads. Each CUDA block is executed by one streaming multiprocessor (SM) and cannot be migrated to other SMs in GPU. Each kernel is executed on one device and CUDA supports running multiple kernels on a device at one time.[43]

Figure 6.6 shows how kernels are executed and mapped onto the GPU's hardware resources. Threads within a block are identified by the built-in 3D variable **threadIdx**. Blocks within a grid are indexed using another built-in 3D variable called **blockIdx**. The dimension of the thread block is accessible within the kernel through the **blockDim**.

The thread index idx is calculated by $i = blockIdx.x * blockDim.x + threadIdx.x$ where $blockIdx.x$ is the x dimension block identifier, $blockDim.x$ is the x dimension of the block dimension and $threadIdx.x$ is the x dimension of the thread identifier. The MCFT1 and MCFT2 algorithms 1 - 2 differ only in computation of F_{X_T}. The simulation parts consisting of interpolation and summation are identical in both methods and can be adapted to run on GPU (algorithm 3).

6.2.4 Results

Algorithm 3 Put option pricing through Inverse sampling on GPU

Input: Number of paths M, CDF F_{X_T}
Output: Option price V_0
Upload F_{X_T} *to GPU*
Initialise the random states in the GPU
On the GPU:
Allocate memory for vectors u,$\hat{x}$ *of size M*
$idx \leftarrow blockIdx.x * blockDim.x + threadIdx.x$
$u[idx] \leftarrow U \sim \text{Unif}[0,1]$
$\hat{x}[idx] \leftarrow F^{-1}_{X_T}(u[idx])$ ▷ Equation 6.3
$V_0 \leftarrow 0$
for $i \leftarrow idx$ to M **do**
$\hat{V}_T \leftarrow \max(K - e^{\hat{x}[i]}, 0)$
$V_0 \leftarrow V_0 + \frac{e^{-rT}}{M}\hat{V}_T$
end for
Download V_0 *from GPU*
return V_0

Three discussed methods together with MCFT1 and MCFT2 were tested for European puts on a collection of three sets of parameters. All three represent processes with infinite activity at $Y > 0$. Under set I the process is of infinite variation at $Y \in (1, 2)$.

For Carr-Madan log-strike spacing was set at $\lambda = 0.0125$ and the damping parameter at $\alpha = 1.5$, the same as under VG. Like in MCFT methods, the interpolation step for Carr Madan and FST consisted of linear interpolation for a more fair comparison. For the COS method simple range of integration (equation 5.18) was used with $L_{COS} = 20$ in set I and $L_{COS} = 10$ in sets II, III. For MCFT-1 same range of integration was used with $L_{COS} = 5$. For MCFT-2 parameter setting was $D = 10$ and $L = 150$. The number of simulations for Monte-Carlo was set at $N_{sim} = 10^6$. Set I is taken from [44], set II from [23], and set III from [29].

I. $S_0 = 10$, $r = 0.1$, $q = 0.0$, $T = 0.25$, $C = 1.0$, $G = 8.8$, $M = 9.2$, $Y = 1.8$

II. $S_0 = 100$, $r = 0.1$, $q = 0.0$, $T = 1$, $C = 1$, $G = 5$, $M = 5$, $Y = 0.5$

III. $S_0 = 100$, $r = 0.04$, $q = 0.0$, $T = 1$, $C = 0.5$, $G = 2.0$, $M = 3.5$, $Y = 0.5$

N	SET 1 pricing time (ms)			SET 2 pricing time (ms)			SET 3 pricing time (ms)		
	CM	FST	COS	CM	FST	COS	CM	FST	COS
512	0.417	19	12	0.391	19	12	0.422	20	12
1024	0.828	39	25	0.782	38	23	0.799	39	24
2048	1.727	79	49	1.635	78	47	1.702	80	49
4096	3.46	160	98	3.35	158	93	3.38	159	95
8192	7.014	330	197	6.873	327	186	6.831	332	191

Table 6.3: Pricing time in milliseconds for different Fourier methods under the CGMY model. In total 50 strikes.

The time complexity of Fourier methods under CGMY (figure 6.7) exhibits the same pattern as under Variance Gamma (figure 6.1). All three implementations depend linearly

on the number of terms N. The intercept value on a log scale is higher for COS and FST since these methods price options individually while Carr Madan handles the whole chain simultaneously.

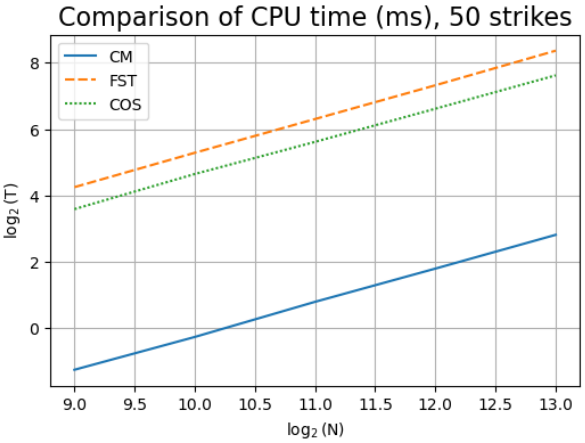

Figure 6.7: Pricing time under CGMY. Datapoints from Table 6.3. Set I.

Figures 6.8-6.10 depict CGMY pricing errors for different sets at $N = 1024$. The Fourier transform-based pricing and MCFT-2 demonstrate consistent oscillation around zero across the strike chain for all three sets. At the same time, MCFT-1 produces error trends toward the ends of the strike chain.

Figure 6.10 shows errors without MCFT-1 for more accurate comparison on a smaller scale. MCFT-2 errors have a magnitude greater by several times that of CM and FST.

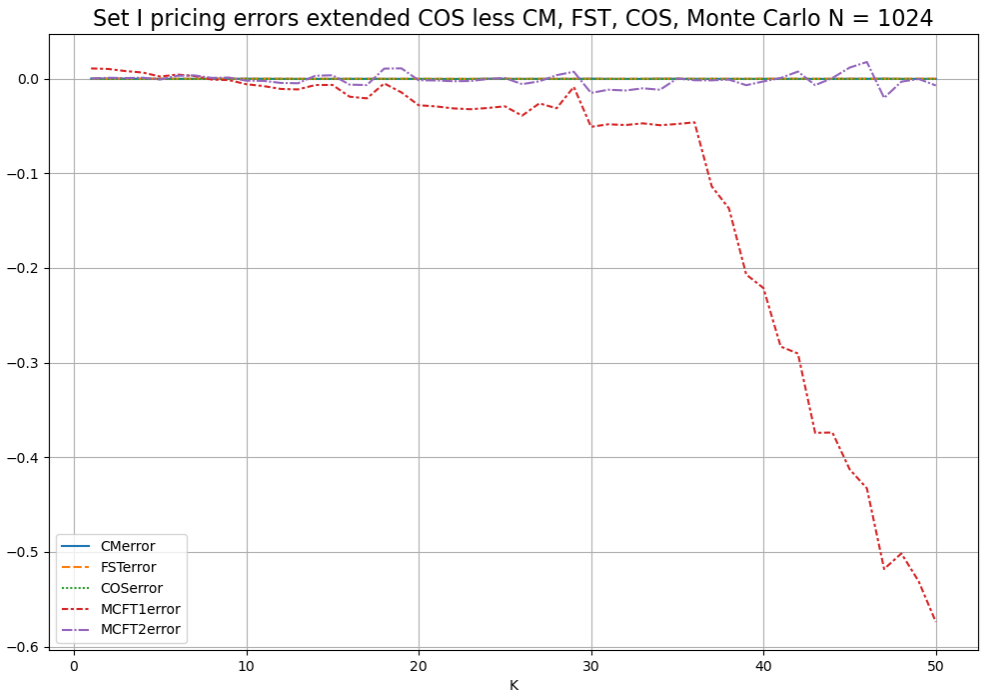

Figure 6.8: Error plot for CGMY model. Number of expansion terms N = 1024. Reference price by COS 5.13 with $N = 2^{14}$. Set I.

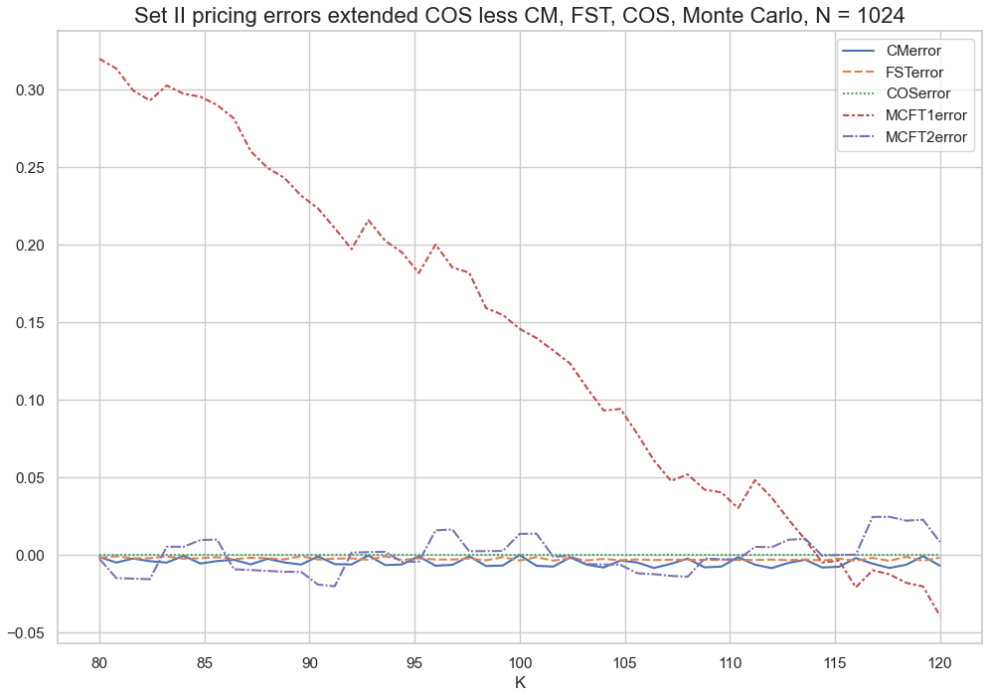

Figure 6.9: Error plot for CGMY model. Number of expansion terms N = 1024. Reference price by COS 5.13 with $N = 2^{14}$. Set II.

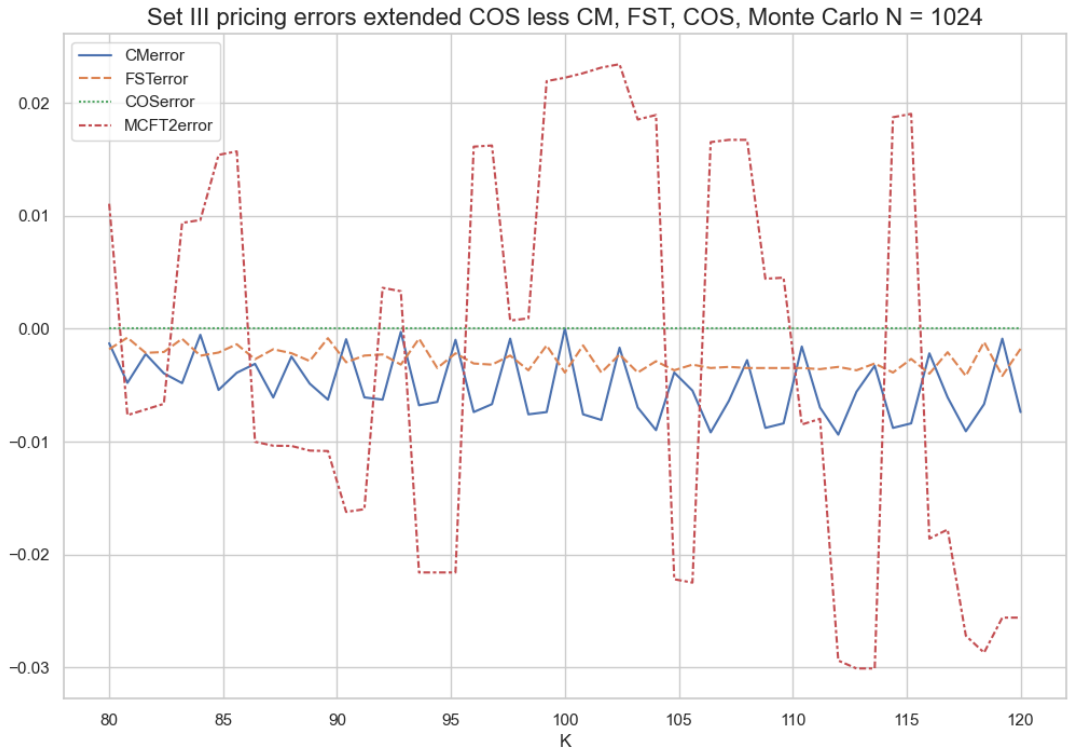

Figure 6.10: Error plot for CGMY model. Number of expansion terms N = 1024. Reference price by COS 5.13 with $N = 2^{14}$. Set III.

N	SET 1 pricing error			SET 2 pricing error			SET 3 pricing error		
	CM	FST	COS	CM	FST	COS	CM	FST	COS
512	41.98	0.0005	0.0000	0.0062	0.0154	0.0000	0.0064	0.0169	0.0000
1024	0.0003	0.0002	0.0000	0.0085	0.0038	0.0000	0.0094	0.0042	0.0000
2048	0.0003	0.0001	0.0000	0.0085	0.001	0.0000	0.0094	0.0011	0.0000
4096	0.0003	0.0001	0.0000	0.0085	0.0003	0.0000	0.0094	0.0003	0.0000
8192	0.0003	0.00001	0.0000	0.0085	0.0001	0.0000	0.0094	0.0001	0.0000

Table 6.4: Maximum pricing error for different Fourier methods under the CGMY model. In total 50 strikes.

As stipulated in COS paper[23], the COS converge exponentially. And since the COS method with $N = 2^{14}$ was used as the reference, it explains zero errors in all three sets. CM exhibits the same trend under CGMY as under VG with MaxError remaining on the same level with greater N. The FST preserved the error reduction trend with larger N.

SET	Monte Carlo pricing error		Time performance (ms)		
	MCFT-1	MCFT-2	MCFT-1	MCFT-2	COS extended
I	0.5584	0.0176	13100	9150	42050
II	0.3196	0.0423	12200	8700	66300
III	0.4207	0.0498	12550	8800	68450

Table 6.5: Maximum pricing error for MCFT-1 and MCFT-2 under the CGMY model. Time performance for Monte Carlo and COS with $N = 2^{14}$. Number of simulations $N_{sim} = 10^6$. In total 50 strikes.

Both Monte-Carlo implementations spent more time to price option chain than any Fourier method and resulted in higher MaxError. It seems the COS method in MCFT-1 does not produce sufficiently accurate values for CDF recovery, which results in a growing bias of price. On the other hand, recovery through the regularized CDF provides consistent values, close to reference prices.

Additional experimentation which is not presented here with a larger number of samples did neither produce lower bias for MCFT-1 nor decreased MaxError for MCFT-2. A more careful parameter selection is required when increasing N_{sim} for the errors to decrease. An additional improvement may be carried out by replacing the linear interpolation in 6.3 with a cubic spline.

Chapter 7

Conclusions

The comparison of Fourier methods highlights the COS method as the best-performing. However, the question of the range of integration presents a major obstacle to the practical application of the COS method. As it has been argued in [26], the method shows sensitivity in the choice of the integration interval for some models like CGMY. The current project did not include the complex integration interval 5.17 and all L_{COS} values were hand-picked manually. Further investigations of the suitability of the COS method for option pricing should be concerned with the question of integration range choice as well as which values of L_{COS} provide better convergence.

As expected, for the option chain pricing the fastest method was Carr Madan since it was run to price the whole chain simultaneously. However, the constant shift from reference values persisted across different numbers of expansions in FFT, different parameter settings, and even different share price models. A possible explanation for this is the interpolation error. The other one is the choice of damping parameter α. It should be noted that α was chosen so that errors under VG are minimized. Further study of different α under CGMY values is required.

The FST method provided consistent error reduction both under VG and CGMY. Despite taking longer time than COS, it has the advantage of being parameter-free with the exception of choice of partition in 4.7. The other advantage is it is easily adapted for exotic options. Note the code for all Fourier methods is not optimal and the comparison is general for the current implementation.

MCFT-1 results prompt to reject current implementation. The growing error toward ITM or OTM regions suggests that "brute" sampling from recovered CDF produces bias of terminal share price. MCFT-2 resulted in consistent prices, however worse than Fourier-based pricing. MCFT-2 depends on the length of the integration interval in real and Fourier Space D and L. In this project, these parameters were set to constant values following example values in [29]. The selection procedure, proposed in [29] was omitted. This is probably the reason for large MaxError values, which do not match results in the

original paper [29]. This is another direction for future research.

The other area for future study is an adaptation to run on the GPU of all studied methods. Running FFT on GPU can speed up FST and CM pricing. The COS method is parallelizable as well[24].

The pricing problem could be extended to the exotic (not European) options. FST and MCFT-2 allow path-dependent option pricing. Also, FST can be adapted to price American options.

References

[1] Louis Bachelier. "Théorie de la spéculation". In: *Annales Scientifiques de l'École Normale Supérieure* 3.17 (1900), pp. 21–86.

[2] Albert Einstein. "Über die von der molekularkinetischen Theorie der Wärme geforderte Bewegung von in ruhenden Flüssigkeiten suspendierten Teilchen". In: *Annalen der Physik* 322.8 (1905), pp. 549–560.

[3] James Owen Weatherall. *The Physics of Wall Street: A Brief History of Predicting the Unpredictable*. Boston, MA: Houghton Mifflin Harcourt, Jan. 2013.

[4] Rama Cont and Peter Tankov. *Financial modelling with jump processes*. Chapman Hall, 2004.

[5] Fischer Black and Myron Scholes. "The Pricing of Options and Corporate Liabilities". In: *Journal of Political Economy* 81.3 (1973), pp. 637–654.

[6] Robert C. Merton. "Theory of Rational Option Pricing". In: *The Bell Journal of Economics and Management Science* 4.1 (1973), pp. 141–183.

[7] Bruno Dupire. "Pricing with a Smile". In: *Risk* 7 (1994), pp. 18–20.

[8] Emanuel Derman and Iraj Kani. "Riding on a Smile". In: *Risk* 7 (1994), pp. 32–39.

[9] Steven L. Heston. "A Closed-Form Solution for Options with Stochastic Volatility with Applications to Bond and Currency Options". In: *The Review of Financial Studies* 6.2 (1993), pp. 327–343.

[10] Robert C. Merton. "Option Pricing when Underlying Stock Returns are Discontinuous". In: *Journal of Financial Economics* 3.1-2 (1976), pp. 125–144.

[11] Steven G. Kou. "A Jump-Diffusion Model for Option Pricing". In: *Management Science* 48.8 (2002), pp. 1086–1101.

[12] Dilip Madan. "Purely Discontinuous Asset Price Processes". In: *Option pricing, Interest rates and risk management* (Oct. 2001), pp. 105–153.

[13] Benoit B Mandelbrot. "Scaling in financial prices. I. Tails and dependence". In: *Quantitative Finance* 1 (2001), pp. 113–123.

[14] Peter Carr et al. “The Fine Structure of Asset Returns: An Empirical Investigation”. In: *The Journal of Business* 75 (2 2002), pp. 305–332.

[15] Dilip B. Madan, Frank Milne, and Hersh Shefrin. “Option pricing with VG martingale components”. In: *Mathematical Finance* 1.4 (1989), pp. 1–21.

[16] Gurdip Bakshi and Zhiwu Chen. “An Alternative Valuation Model for Contingent Claims”. In: *Journal of Financial Economics* 44.1 (1997), pp. 123–165.

[17] Julian Gil-Pelaez. “Note on the inversion theorem”. In: *Biometrika* 38.3-4 (1951), pp. 481–482.

[18] Peter Carr and Dilip Madan. “Option valuation using the fast Fourier transform”. In: *Journal of Computational Finance* 2.4 (1999), pp. 61–73.

[19] Alan Lewis. “A Simple Option Formula for General Jump-Diffusion and Other Exponential Levy Processes”. In: *SSRN Electronic Journal* (May 2002).

[20] R. Lord et al. “A Fast and Accurate FFT-Based Method for Pricing Early-Exercise Options under Lévy Processes”. In: *SIAM Journal on Scientific Computing* 30.4 (2008), pp. 1678–1705.

[21] Kenneth Jackson, Sebastian Jaimungal, and Vladimir Surkov. “Fourier Space Time-Stepping for Option Pricing With Levy Models”. In: *Journal of Computational Finance* 12 (2 Mar. 2007), pp. 1–29.

[22] Vladimir Surkov. “Parallel option pricing with Fourier space time-stepping method on graphics processing units”. In: *Parallel Computing* 36.7 (2010), pp. 372–380.

[23] F. Fang and C. W. Oosterlee. “A Novel Pricing Method for European Options Based on Fourier-Cosine Series Expansions”. In: *SIAM Journal on Scientific Computing* 31.2 (2009), pp. 826–848.

[24] Bowen Zhang and Cornelis W. Oosterlee. “Option pricing with COS method on graphics processing units”. In: *IPDPS ’09* (2009), pp. 1–8.

[25] A. -M. Matache, P. -A. Nitsche, and C. Schwab. “Wavelet Galerkin pricing of American options on Levy driven assets”. In: *Quantitative Finance* 5.4 (2005), pp. 403–424.

[26] Luis Ortiz-Gracia and Cornelis W. Oosterlee. “Robust Pricing of European Options with Wavelets and the Characteristic Function”. In: *SIAM Journal on Scientific Computing* 35.5 (2013), pp. 1055–1084.

[27] Stef Maree, Luis Ortiz Gracia, and Kees Oosterlee. “Fourier and wavelet option pricing methods”. In: *High-Performance Computing in Finance: Problems, Methods, and Solutions* (Feb. 2018), pp. 249–272.

[28] Dilip B. Madan, Peter P. Carr, and Eric C. Chang. “The Variance Gamma Process and Option Pricing”. In: *Review of Finance* 2.1 (Apr. 1998), pp. 79–105.

[29] Laura Ballotta and Ioannis Kyriakou. “Monte Carlo Simulation of the CGMY Process and Option Pricing”. In: *Journal of Futures Markets* (Jan. 2014), pp. 1095–1121.

[30] Wenting Chen, Meiyu Du, and Xiang Xu. “An explicit closed-form analytical solution for European options under the CGMY model”. In: *Communications in Nonlinear Science and Numerical Simulation* 42 (2017), pp. 285–297.

[31] Steven E. Shreve. *Stochastic Calculus for Finance II: Continuous-Time Models*. New York, NY: Springer, 2004.

[32] Cornelis W. Oosterlee and Lech A. Grzelak. *Mathematical Modeling and Computation in Finance: With Exercises and Python and Matlab Computer Codes*. World Scientific, 2020.

[33] John Hull. *Options, futures, and other derivatives*. 9th ed. Boston, Mass: Pearson, 2017.

[34] Wim Schoutens, Erwin Simons, and Jurgen Tistaert. “A Perfect Calibration! Now What?” In: *Wilmott* 2004 (Mar. 2004).

[35] Mark S. Joshi. *More Mathematical Finance*. Pilot Whale Press, 2011.

[36] Ekaterina Voltchkova and Rama Cont. “Integro-Differential Equations for Option Prices in Exponential Lévy Models”. In: *Finance and Stochastics* 9 (Feb. 2005), pp. 299–325.

[37] Gustav Ludvigsson. “Numerical Methods for Option Pricing under the CGMY Process”. M.Sc. thesis. Uppsala University, 2015. URL: `https://urn.kb.se/resolve?urn=urn:nbn:se:uu:diva-252415`.

[38] ManWo Ng. “Option Pricing via the FFT”. M.Sc. thesis. Applied Institute of Mathematics, TU Delft, 2005.

[39] Vladimir Surkov. `http://individual.utoronto.ca/vsurkov/research/fst.html`.

[40] Boost C++ Libraries. `https://www.boost.org/`. Version 1.85.0. 2024.

[41] Tino Kluge. `https://kluge.in-chemnitz.de/opensource/spline/`.

[42] Boost C++ Libraries. `https://beta.boost.org/doc/libs/1_82_0/libs/math/doc/html/math_toolkit/pol_tutorial/policy_tut_defaults.html`. Version 1.85.0. 2024.

[43] Pradeep Gupta. `https://developer.nvidia.com/blog/cuda-refresher-cuda-programming-model/`.

[44] Iris Wang, Justin Wan, and Peter Forsyth. “Robust Numerical Valuation of European and American Options Under the CGMY Process”. In: *Journal of Computational Finance* 10 (Apr. 2007).